Catena 260 (2025) 109454

Contents lists available at ScienceDirect

Catena

journal homepage: www.elsevier.com/locate/catena

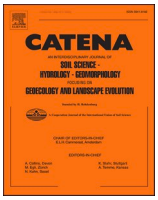

Patterns and thresholds for soil pH across Europe in relation to soil health and degradation

Inma Lebron [a,*], Christopher J. Feeney [a], Sabine Reinsch [a], Nima Shokri [b,c], Mehdi H. Afshar [b,c], Steve Lofts [d], Rob Griffiths [e], David Fidler [e], Briony Jones [a], Panos Panagos [f], Kasia Sawicka [a], Aidan M. Keith [d], Fiona Seaton [d], David A. Robinson [a]

[a] UK Centre for Ecology & Hydrology, Environment Centre Wales, Deiniol Road, Bangor LL57 2UW, UK
[b] Institute of Geo-Hydroinformatics, Hamburg University of Technology, Hamburg, Germany
[c] United Nations University Hub On Engineering to Face Climate Change at the Hamburg University of Technology, United Nations University Institute for Water, Environment and Health (UNU-INWEH), Hamburg, Germany
[d] UK Centre for Ecology & Hydrology, Library Avenue, Bailrigg, Lancaster LA1 4AP, UK
[e] School of Natural Sciences, Bangor University, Bangor, United Kingdom
[f] European Commission, Joint Research Centre (JRC), Ispra, Italy

A B S T R A C T

Soil pH indicates the level of acidity or alkalinity in the soil environment, influencing various biogeochemical and physical processes. Additionally, soil pH levels are crucial in determining the bioavailability of elements such as iron, aluminium, and heavy metals which can be harmful. As such, pH is an important soil health and degradation indicator. Although there is a well-established understanding of soil pH at localized levels, the spatial and temporal variations, as well as significant thresholds at national and continental scales, are not sufficiently documented. Here we analyse the European topsoil pH data (LUCAS) in combination with other soil properties from the LUCAS survey, to identify thresholds and spatial patterns of soil pH across Europe in relation to soil health and degradation. At the European scale we found: 1) the water balance, calculated as mean annual precipitation minus potential evapotranspiration (MAP-PET), provides essential context to interpret soil pH; 2) the shift from organic carbon-rich soils to those dominated by inorganic carbon is observed at a pH of about 7.2, however, soil moisture levels may be more critical than pH for the accumulation of soil organic carbon; 3) we identified three distinct clusters within the multivariate regression tree: acidophiles (below pH 5.2), neutrophiles (pH 5.2–6.9) and alkaliphiles (above pH 6.9), while optimum microbial diversity occurred between pH 6 and 7. Earthworm abundance, as reported by the sWorm database, is more nuanced and dependent on land use; 4) risk of degradation by heavy metals cannot be captured by a single pH threshold. Finally, we identify soil pH thresholds that can aid policymakers in identifying regions that may require protection or intervention.

1. Introduction

Soils serve as a fundamental element of ecosystems, providing a range of services that are crucial for human well-being and environmental sustainability (Fernandez-Ugalde et al., 2022). Considerate management and conservation of soils are vital for maintaining these ecosystem services and their associated benefits. One indicator affecting ecosystem services is soil pH, which was identified as a critical indicator of soil quality (Bünemann et al., 2018). It is one of the twelve soil descriptors employed to assess soil health in the European Union, as stipulated by the proposal for an EU Soil Monitoring and Resilience Law (European Commission, 2023) and it is among the eight indicators to track changes during the Soil Mission implementation (Panagos et al., 2024).

It has long been recognised that the measurement of pH in the soil solution is an important integrating measure of element and nutrient availability (Hartemink and Barrow, 2023) as it regulates the soils capacity to store and supply nutrients. Soil pH plays a critical role in modulating soil organic matter dynamics and regulates the availability of macro- and micro-nutrients, with direct implications for crop production and food security (Hou, 2023; Pozza and Field, 2020). Furthermore, pH regulates various biological processes and the activities of soil microorganisms (Malik et al., 2018), which is particularly important given that soils support 59 % of species on Earth (Anthony et al., 2023). The community of soil bacteria, particularly those responsible for organic matter decomposition and nitrogen fixation, is optimally adapted to the pH levels typically found in their natural environments (Fernández-Calviño and Bååth, 2010). When pH levels shift, these microorganisms initiate an adaptive response characterized by the production of exoenzymes to accommodate the change (Puissant et al.,

* Corresponding author.
E-mail address: inmbin@ceh.ac.uk (I. Lebron).

https://doi.org/10.1016/j.catena.2025.109454
Received 20 May 2025; Received in revised form 20 August 2025; Accepted 10 September 2025
Available online 30 September 2025

2019). Research has shown that bacterial diversity and richness in soils tend to peak at pH levels between 6 and 7 (Chu et al., 2010; Fierer and Jackson, 2006; Tripathi et al., 2012). Consequently, measuring soil pH is a vital indicator for evaluating soil health and its capacity to support plant growth (Neina, 2019), as well as its overall ecosystem functionality and implications for human health (McBride, 1994).

While pH is essential for soil health, it also indicates land degradation and the potential to harm organisms. Soil pH significantly affects the accumulation, mobility, and bioavailability of metals and heavy metals, which can create toxic conditions for various plants and organisms (Lofts, 2022). For example, in the 1970 s, air pollution across Europe led to increased soil acidity and forest decline (Smith et al., 2024). Although recovery in Britain's soils was observed due to policy interventions (Reynolds et al., 2013), more recent monitoring indicates this has slowed or potentially reversed, likely as a result of climate drivers or land use management pressures (Seaton et al., 2023). Given the important role soil pH plays in element cycling and plant productivity, it is carefully managed in agricultural and horticultural habitats. Acid soils are often limed to raise their pH and alkaline soils can have sulphur added to reduce their pH. Another often-overlooked aspect of potential for degradation is the influence of pH on soil structural stability; the interaction between pH and alkaline cations, particularly sodium, can lead to clay dispersion and can exacerbate erosion (Shainberg and Levy, 2020). The degradation of the natural habitat, where biological activity occurs, may further impair the delivery of ecosystem services by reducing the available niche space associated with soil structural diversity (Seaton et al., 2020).

Parent material plays an important role in pH at large scales, especially in the initial stages of soil formation, but vegetation and climate quickly modify soil pH levels. Recent research on soil pH shows that global patterns of soil pH are related to biomes and to the mean annual precipitation (MAP) and mean annual temperature (MAT) (Zhao et al., 2019). Global soil pH patterns were shown to be fundamentally linked to the water balance with regional modifications due to parent material (Slessarev et al., 2016). A transition point was shown to exist at the global scale where MAP exceeds mean annual potential evapotranspiration (PET) (Slessarev et al., 2016); wet soils being more acidic and dry soils being more alkaline. It is well known that environmental forcing regulates many aspects of soil chemistry, including pH (Jenny, 1994). However, it is only recently, with our ability to aggregate large global data sets, that the patterns which emerge across scales can be quantified and attributed to different environmental drivers. Climate through water balance, parent material (Slessarev et al., 2016), and land management type drives large scale patterns, whilst pressures such as pollution and specific management practices superimpose effects at local scales.

One of the significant challenges encountered is the interpretation of pH changes, particularly the need to differentiate the effects of various large- and small-scale drivers and pressures. Overcoming these challenges will help to comprehend, and ultimately forecast, the consequences of environmental change. Our aim is to adopt a comprehensive approach to identify pH thresholds, optima or changes that are pertinent for informing policy decisions at both national and European levels. This paper investigates the large-scale pH patterns across Europe as reported by the Land Use/Cover Area frame statistical Survey (LUCAS) for soils sampled in 2018 (Orgiazzi et al., 2018), beginning with fundamental geochemical relationships and progressing to the implications for nutrients, micronutrients, and metal toxicity. Additionally, we examine the connections between biota, land use, and microbial and worm abundance in relation to pH. Through this analysis, we aim to uncover consistent patterns and critical thresholds in a holistic way for interpreting pH as an indicator of soil health and degradation in the context of environmental change throughout Europe. The specific goals of this study include (i) determining if the water balance creates thresholds in soil pH in European topsoils; (ii) to identify thresholds associated with carbon storage and the transition from soil organic carbon (SOC) to soil inorganic carbon (SIC); (iii) to determine the optimal pH for microbial diversity and worm abundance in European soils; and (iv) to analyse spatial patterns of the susceptibility of soils to heavy metal release as influenced by soil pH.

2. Material and methods

2.1. European soil pH and carbon data

Approximately 19,000 soil samples from the topsoil (0–20 cm) in georeferenced locations from across 27 countries in the European Union plus the UK were collected in 2018 by the Land Use and Cover Area Frame Survey (LUCAS) (Orgiazzi et al., 2018; Fernandez-Ugalde et al., 2022). We mapped pH data using R version 4.5.1 using the "tidyterra" package by Hernangómez (2023). From the parameters measured in the soils we examined the pH data and the organic and inorganic carbon concentrations. Measurements of pH were performed in a 1:5 soil: deionized water ratio according with the method ISO 10390:2005 (data shown in Fig. 1). Organic carbon was analysed by dry combustion following the ISO 10694:1995 and carbonated by the volumetric method, ISO:10693:1995. Maps showing the spatial distribution of organic matter based on LUCAS data have been reported by Castaldi et al., 2019. The crossover between the decrease of SOC and increase of SIC with pH increasing, was modelled as functions of soil pH using a non-linear quantile regression model, which assumes a sigmoid relationship in both scenarios (Andersen (2002), eq. S1).

2.2. Climate data

Data on mean annual precipitation (MAP) and mean monthly potential evapotranspiration (PET) at a resolution of 1 km for the period from 1981 to 2010 were obtained from the CHELSA climate data repository. MAP and PET were extracted to the locations of sampling points from the LUCAS 2018 survey using the "extract" function from the "terra" package (Hijmans, 2020) in R (Team, 2024). Monthly PET was multiplied by 12 to estimate annual values before subtracting from MAP and dividing by 1000 to get the water balance in metres. Scatter plots were generated in R using the "ggplot2" package (Wickham and Wickham, 2016) to show the relationship between MAP-PET and soil pH (in water). Histograms of pH and MAP-PET values were plotted using the "ggMarginal" function from the "gridExtra" package (Auguie and Antonov, 2017).

2.3. DNA (microbiome), bioinformatics and statistical analysis

The LUCAS 16S rRNA gene sequences were processed using nf-core/ampliseq version 2.9.0 (da Veiga Leprevost et al., 2017; Ewels et al., 2020; Grüning et al., 2018; Straub et al., 2020). Adapter and primer sequences were trimmed using Cutadapt 4.6 (Martin, 2011) and all untrimmed sequences were discarded. Sequences were then processed sample-wise (independent) with DADA2 1.30.0 (Callahan et al., 2016) to eliminate PhiX contamination, trim reads (before median quality drops below 25 and at least 75 % of reads are retained; forward reads at 219 bp and reverse reads at 216 bp, reads shorter than this were discarded), discard reads with $>$ 2 expected errors, correct errors, merge read pairs, and remove polymerase chain reaction (PCR) chimeras. This produced 145,714 amplicon sequencing variants (ASVs) across the 881 LUCAS 16S rRNA libraries. Taxonomic classification was performed by DADA2 using the Silva 138.1 database (Quast et al., 2012). ASVs with taxonomic assignments of 'mitochodria' and 'chloroplast' were excluded from any further analyses, giving a final total of 143,893 ASVs. Singleton taxa were removed prior to statistical analyses, samples with a sequencing depth of less than 5000 reads were discarded. Where duplicate samples were present, the duplicate with the greatest number of reads was retained. Reads were rarefied to 5000 across samples using the Vegan package to account for variable sequencing depth. To identify

outlier samples decorana scores were calculated, euclidean distances were determined between sample axis scores and the mean scores of each ordination axis, samples with an euclidean distances greater than the 99th percentile were removed. Loess regression was used to assess the relationship between Shannon's diversity and soil pH, a pH optimum relating to diversity was identified at the soil pH with the maximum loess fitted Shannon's diversity. To evaluate pH associated shifts in bacterial community composition, multivariate regression tree analysis was carried out on the proportional abundance compositional matrix - after rarefaction to 5000 reads per sample using the mvpart library in R.

2.4. European earthworm data

Data on earthworm abundance relevant to the European Union were sourced from the sWorm database (Phillips et al., 2021) and modelled using Generalised Additive Models (GAMs). The database was specifically filtered to include only European countries and to select data points where both earthworm abundances and soil pH were documented, resulting in a subset dataset of 1,348 records. It covered 20 European countries having a good representation across latitude and climatic zones (Table 1). Only those methodologies that involved hand sorting were considered, leading to the exclusion of a further 104 records. We standardized land use information provided in the sWorm database (Land use, Habitat cover, Management system, and habitat as described) into LUCAS equivalent land cover categories, namely Croplands, Grasslands, and Woodlands, which resulted in 1,177 usable data points. A series of General Additive Models (GAMs, utilizing the 'mgcv' package version 1.9–1 (Wood, 2011) were employed, incorporating random factors including Extraction Method, Country, and the month when data collection concluded, serving as indicators of sampling timing. The Akaike information criteria (AIC), an estimator of prediction error, was used to gauge the relative quality of the statistical model for the data, with the smaller number indicating a more accurate model. The dataset used included 569 datapoints for Cropland, 187 datapoints for grassland and 424 datapoints for grassland. The functions plot_predictions and plot_slopes from the 'marginaleffects' package (Arel-Bundock et al., 2024) were utilized to visualize predictions of earthworms' abundance, or first derivative, across the range of pH values.

2.5. Computation and mapping of the metal vulnerability in EU soils

The assessment of metal leaching risk from soils, or the vulnerability index, was determined for European soils using LUCAS data and the POSSMs model (Supplementary Methods) (Lofts, 2022). We forecasted the alterations in concentrations of nickel, copper, zinc, and cadmium in porewater resulting from changes in soil conditions, such as increased moisture from precipitation over short durations of a few days. It comprises dissolved metal in porewater, and adsorbed metal bound to chemically active soil components. The POSSMs model is an equilibrium chemical speciation model for soils that requires minimal input for computations and is thus useful for large scale application. The vulnerability index is centred on the reaction of metal concentration in the soil porewater to the introduction of metal in a 'reactive' state. The reactive metal represents the fraction of metal that quickly adjusts to variations in soil conditions and governs the concentration of metal present in the soil porewater.

For each soil, two calculations of the equilibrium distribution of the reactive metal between the soil solids and the porewater are done. The equilibrium distribution using the POSSMs model (Lofts, 2022). POSSMs requires the porewater pH, soil organic matter (SOM) content and the concentration of dissolved organic matter (DOM) in the soil porewater.

The porewater metal concentration, $[M]_{pw,POSSMs}$, is first computed for a specific reactive metal concentration, $\{M\}_{react}$. Then, a second simulation is done with the reactive metal content, $\{M\}_{react,aug}$, initially increased (augmented) by 10 %. Before calculation of the porewater concentration, the additional metal is assumed to undergo 'aging' for one year. Aging is a generic term for processes that remove metal from the reactive pool into an unreactive, or 'aged' pool. Unreactive metal does not form part of the pool that can equilibrate with the porewater and thus loss of metal from the reactive pool by aging reduces the modelled porewater concentration. Aging is modelled by reversible first order kinetics, where one or both of the forward or backward rate constants is a function of the porewater pH (Table 2). The porewater metal concentration, $[M]_{pw,POSSMs,aug}$, is then calculated from the sum of the original reactive metal concentration plus the portion of the 10 % additional reactive metal that has not aged.

The vulnerability index is given by the expression

$$vul.index = \frac{\frac{[M]_{pw,POSSMs,aug}}{[M]_{pw,POSSMs}} - 1}{\frac{\{M\}_{react,aug}}{\{M\}_{react}} - 1} \quad (1)$$

If the increase in the reactive metal concentration were to cause the predicted porewater concentration to rise by the same proportion, the vulnerability index would be at its maximum value of unity. Similarly, no change in the predicted porewater concentration would give a vulnerability index of zero. Therefore, the index provides an internally consistent, bounded value that reflects the ability of the soil to buffer metal addition and limit the corresponding increase in the porewater concentration and thus the risk of dissolved metal leaching to groundwater or surface water.

The modelling requires the following dataset for a soil: porewater pH, SOM content (% w/w), porewater DOM (mg L^{-1}), reactive metal concentration (mol g^{-1}).

Porewater pH and SOM content were sourced from the LUCAS 2018 dataset (Fernandez-Ugalde et al., 2022). Only soils sampled from 0 to 20 cm depth were used in computations. Porewater pH (pH_{pw}) was estimated from the pH measured in aqueous soil slurries (pH_H2O) using an expression provided by de Vries et al. (2005):

$$pH_{pw} = -0.2847 + 1.0462 \cdot pH_{H_2O} \quad (2)$$

Porewater DOM was taken from the modelled dataset of (Langeveld

Table 1
Overview of European countries and sample numbers (N) in the sWorm database (Phillips et al., 2021) which had earthworm abundance and pH data associated with them, and where a land cover equivalent to the LUCAS land cover categories could be assigned.

Country	N	Country	N
Austria	3	**Lithuania**	16
Belgium	4	**Netherlands**	124
Denmark	5	**Poland**	55
Finland	167	**Portugal**	74
France	65	**Romania**	34
Germany	257	**Slovakia**	13
Greece	27	**Spain**	61
Hungary	3	**Sweden**	62
Ireland	102	**Switzerland**	4
Italy	36	**United Kingdom**	68

Table 2
First order forward and backward aging rate constants for nickel, copper, zinc and cadmium.

Metal	$\log_{10}$ forward rate constant for aging (d^{-1})	$\log_{10}$ backward rate constant for aging (d^{-1})	Reference
Nickel	$-1.9 + 0.000309e^{pH}$	-1.5	Lofts, unpublished data
Copper	$-2.5 + 0.000501e^{pH}$	$-2.1 + 0.000316e^{pH}$	Xu et al. (2016)
Zinc	$-4.2 + 0.26pH$	-3.2	Xu et al. (2016)
Cadmium	$-2.9 + 0.18pH$	-2.1	Xu et al. (2016)

et al., 2020).

Reactive metal concentrations were measured in the LUCAS 2009/12 survey, but were never published in a publicly accessible dataset, so estimates were made using available maps of total concentrations available on the ESDAC website:Nickel: Tóth et al. (2016), Copper: Ballabio et al. (2018), Zinc: Tóth et al. (2016); Van Eynde et al. (2023), and Cadmium: Ballabio et al. (2024).

Mapped metal concentrations extracted to sample locations in the LUCAS 2018 dataset were used to estimate reactive metal content, based on a set of empirical relationships obtained from paired total and reactive metal concentrations measured by Garforth (2015). The reactive metal concentration is predicted from the total metal concentration using the expression:

$$\{M\}_{react} = K_{tl} \cdot a_H^{\beta_0} \{SOM\}^{\beta_1} \{M\}_{total}^{\beta_2} \quad (3)$$

where $\{M\}_{react}$ and $\{M\}_{total}$ are the reactive and total metal concentrations respectively (mol g^{-1}), a_H is the proton activity in the porewater ($a_H = 10^{-pH_{pw}}$), $\{SOM\}$ is the soil organic matter content (% w/w) and K_{tl}, β_0, β_1 and β_2 are fitted parameters (Table 3).

European vulnerability indices maps were produced for nickel, copper, zinc and cadmium and for soil pH higher and lower than 6 using R version 4.5.1 using the "tidyterra" package by Hernangómez (2023). using R software.

3. Results

3.1. Geochemical buffering

The spatial distribution of pH values across the European continent is illustrated in Fig. 1, with data sourced from the LUCAS 2018 monitoring program.

Combining pH data with meteorological data we obtained Fig. 2, which illustrates the distribution of pH values in relation to the mean annual precipitation (MAP) minus the potential evapotranspiration (PET) across Europe. The blue horizontal lines indicate the upper geochemical threshold for $CaCO_3$ buffered soils, approximately pH 8.2, while the lower red line denotes the geochemical threshold for $Al(OH)_3$ buffered soils, around pH 5.1, below which aluminium species become more prevalent in the soil solution. Fig. 1A encompasses all LUCAS data (n = 19,000), whereas Fig. 1B reflects the LUCAS data for seminatural habitats (woodlands, grasslands, shrublands and wetlands), after excluding agricultural habitats, cropland, and livestock pasture (n = 7157). The histogram in Fig. 1A reveals that when all data is included, the pH distribution peaks at roughly pH 8, followed by a uniform distribution of samples within the neutral and acidic ranges. In contrast, after the exclusion of agricultural habitats, the pH histogram in Fig. 1B exhibits a bimodal distribution with peaks around pH 7.5 and 4.5.

3.2. Acid soils and alkaline soils in Europe

Soils exhibiting pH values below 5.1 and above 8.2 are depicted in Figs. 3A and 3B, respectively. Besides the evident north–south gradient, soils along the western coast are significantly more acidic, particularly in regions with higher moisture, even in southern areas like Portugal. Alkaline soils are primarily found in countries such as Spain, southern France, Italy, Croatia, and extending into Greece. In contrast, there are very few instances of alkaline soils in the northern regions, likely only occurring due to the influence of calcareous parent material such as bands of chalk overshadowing climatic factors. A notable observation is the widespread occurrence of acidic soils across Europe. Approximately 24.1 % of the 19,000 LUCAS samples recorded pH values below 5.1, which suggests a risk of aluminium toxicity. While the pH distribution appears irregular in central Europe, most soils in Scandinavia exhibit pH levels below 5.1, reflecting the predominance of organic soils in those areas. Conversely, only 3.3 % of the sampled soils had pH values exceeding 8.2, most of these occurring in the Mediterranean countries.

Table 3
Parameters for the relationship between total and reactive metal concentrations in soils.

Metal	log K_{tl}	β_0	β_1	β_2	SE (log $\{M\}_{react}$)
Nickel	−1.61		0.732	1.03	0.32
Copper	−1.01	−0.0640		0.990	0.26
Zinc	−0.738		0.585	1.12	0.43
Cadmium	−2.49	−0.105	0.453	0.863	0.36

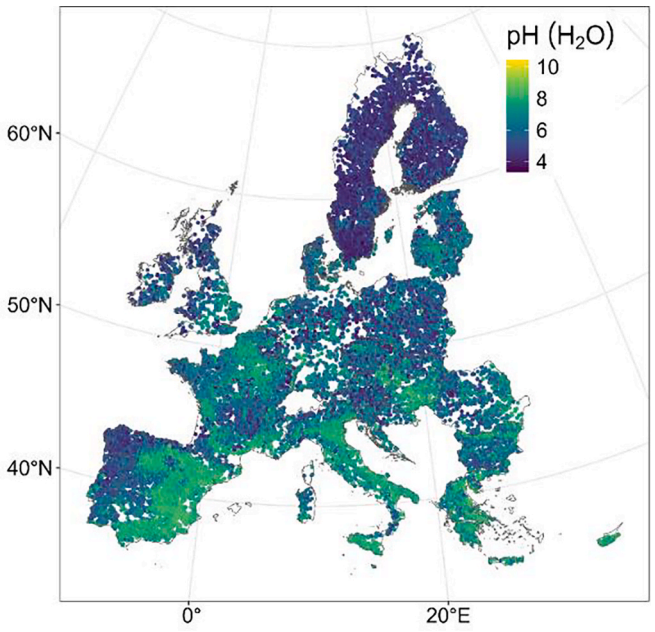

Fig. 1. Distribution of pH in Europe according to the monitoring program LUCAS for the year 2018 data.

3.3. Soil organic carbon (SOC) and soil inorganic carbon (SIC) transition

The relationship between carbon concentration and soil pH, highlighting both SOC and SIC (SIC represented by calcite concentration) is shown in Fig. 4. Fig. 4 illustrates that organic soils are associated with low pH levels, whereas soils rich in carbonates correspond to elevated pH levels across the EU. This observation suggests a significant correlation between SOC and SIC between pH levels 6 to 8. The crossover point, where carbon storage in the forms of SOC and SIC are equally likely, is found to be between pH 7.15 and 7.3, depending on the chosen percentile for SIC.

Fig. 5A illustrates soil organic carbon levels in Europe in relation to the annual water balance (MAP-PET). The point where MAP minus PET equals zero indicates that for soils to accumulate SOC stocks exceeding 200 g kg-1 in the top 0–20 cm, there must be a surplus of MAP compared to PET. In contrast, Fig. 5B indicates that for carbonates to remain stable, PET typically must exceed the MAP.

3.4. pH and the microbiome

To assess the influence of soil pH on soil bacterial communities, and specifically identify thresholds, we used soil data (Fernandez-Ugalde et al., 2022) and 16S rRNA gene sequence molecular data (Labouyrie et al., 2023). An analysis of a subsample of survey points derived from the 2018LUCAS survey data was conducted to assess DNA. The findings illustrated in Fig. 6A, which shows that Shannon's diversity in relation to soil pH, and by land use. The LUCAS data reveals a broad increasing

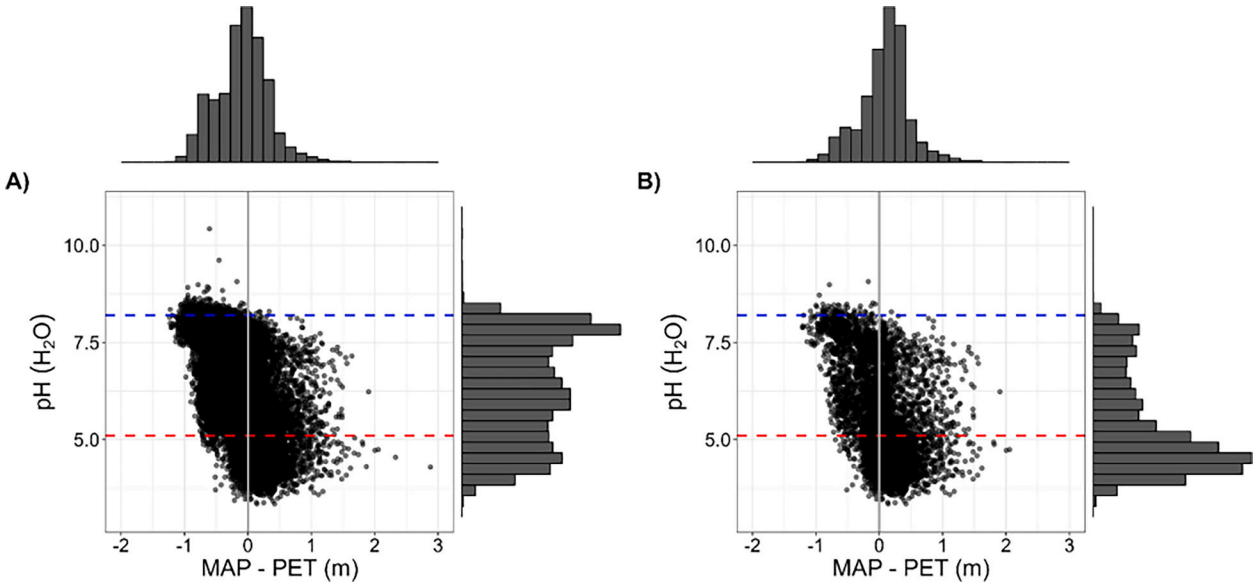

Fig. 2. A) The relationship between topsoil pH (0–20 cm) and annual water balance (MAP-PET) is illustrated using the European dataset from LUCAS 2018, which encompasses approximately 19,000 soil sample measurements. The side panels display histograms depicting the difference between mean annual precipitation (MAP) and potential evapotranspiration (PET), and soil pH values. The blue and red lines indicate the predicted pH levels for soils buffered with $CaCO_3$ (8.2) and $Al(OH)_3$ (5.1), respectively. Graph B) shows the same graph specifically for seminatural habitats ((woodlands, grasslands, shrublands and wetlands), comprising a sample size of 7,157.

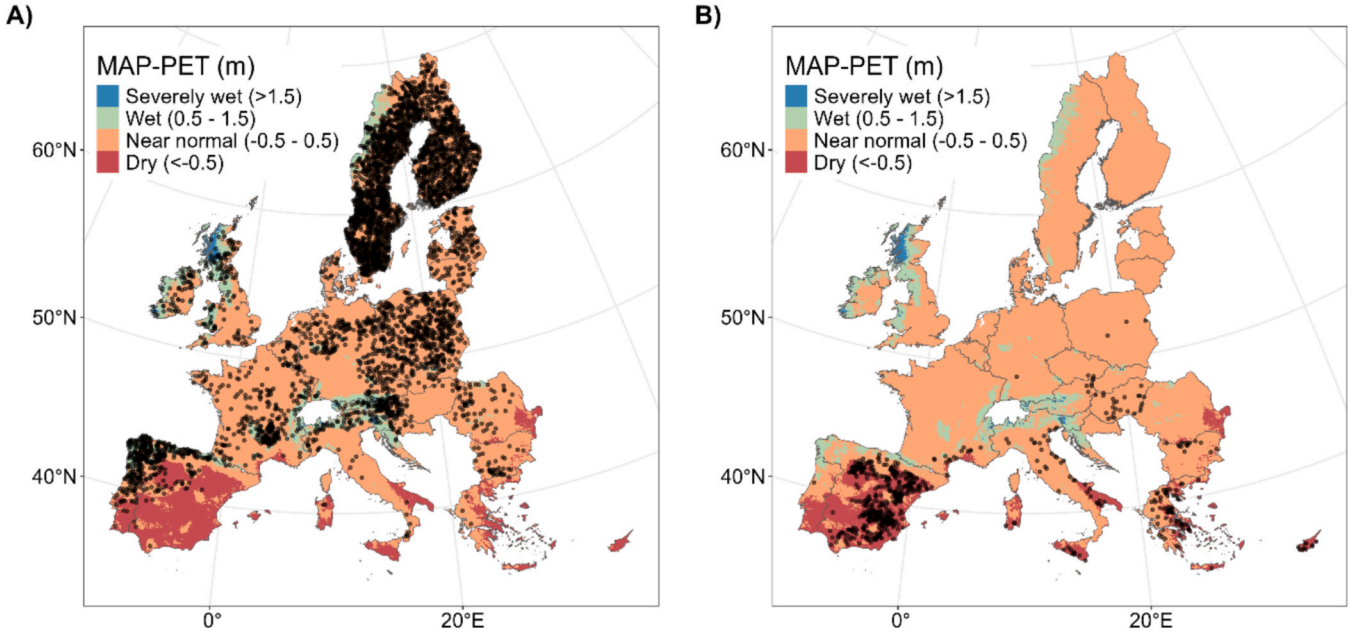

Fig. 3. Panels A and B shows the European map colour coded according to four classes of rain regime from severely wet to dry. Overlapped black dots represent the spatial distribution of soils with pH < 5.1 (A) and > 8.2 (B).

trend with pH peaking at a pH of 6.28, as shown in Fig. 5A. Further analyses of LUCAS compositional microbiome data, using a multivariate regression tree with pH alone as a predictor (Griffiths et al., 2011) (Fig. 6B) identifies distinct community groups clustered according to pH thresholds. One community with a pH below 5.2, another within the pH range of 5.2 to 6.9, and a third that thrives at pH levels above 6.9. The data broadly split into three groups, consistent with acidophiles, neutrophiles and alkaliphiles. Inset barplots reveal higher abundances of Acidobacterial taxa below pH 5.2, which decline at higher pH being replaced by a more even distribution of diverse lineages.

3.5. Earthworms

European data from the sWorms database (Phillips et al., 2021) reveal that earthworms inhabit soils with pH levels ranging from 2.9 to 8.64, averaging 6.05 and with a median of 6.18. (Table 4 and 5 and Figs. 7 and 8). The lowest pH of 2.9 was observed in woodland environments, and all land uses contained earthworm counts at pH levels above 8. The predicted distribution of earthworm abundance varies across the pH range differently for the three land uses (Fig. 9). In woodlands, there is no specific pH threshold; rather, abundance increases in a linear fashion as pH rises.

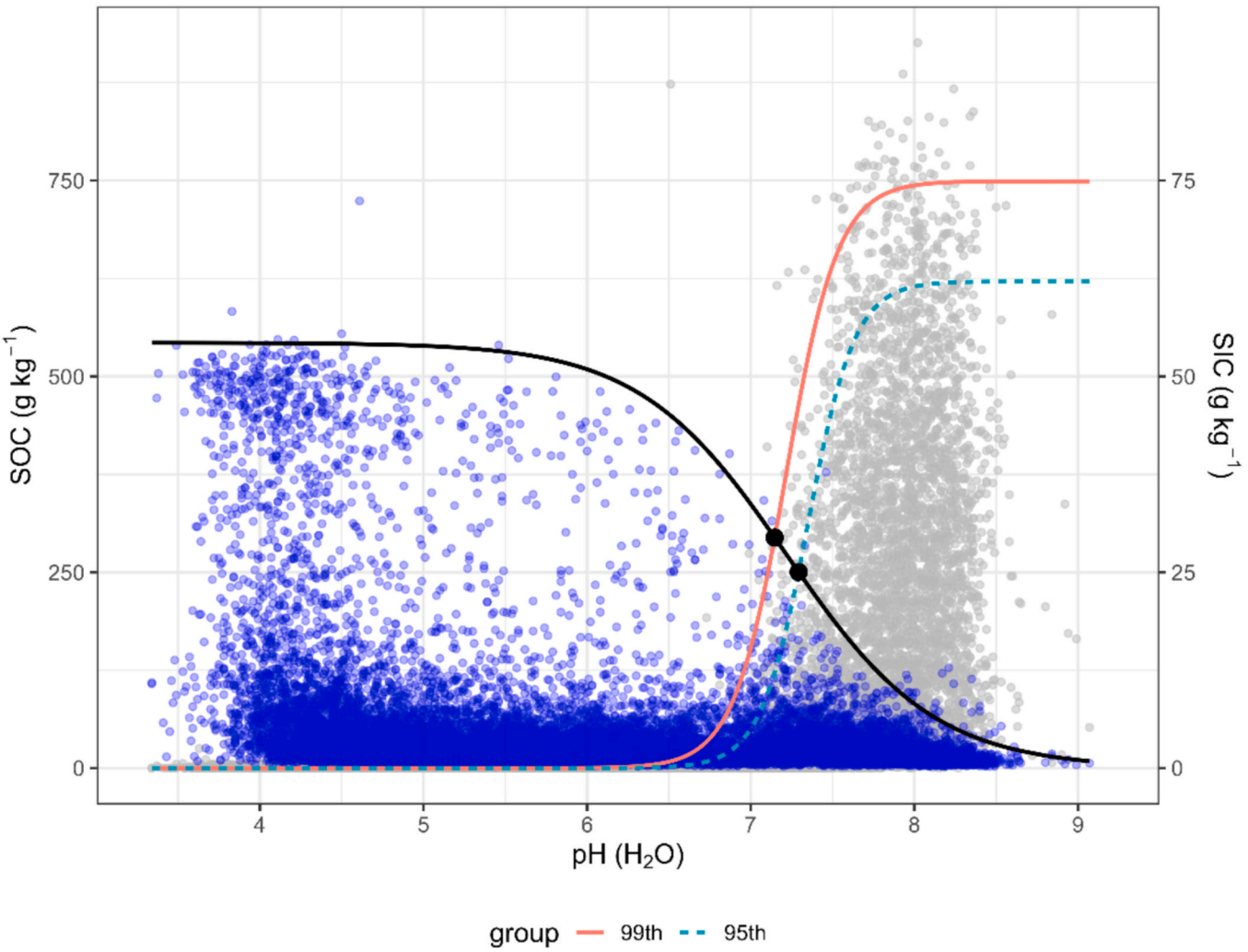

Fig. 4. Soil carbon concentration as a function of pH with soil organic carbon (SOC) and soil inorganic carbon (SIC) transition at a pH of 7.15 (red line) for the European LUCAS 2018 data (when the 99th percentile of the SIC data was considered).

The density of data at low pH values (Fig. 7) likely reflect coniferous woodlands or other woodlands on soil high in SOC. Grasslands exhibit unimodal change with increasing pH reaching their highest predicted earthworm abundance at a pH of 5.95, while cropland exhibits a bimodal pattern, with abundance peaks predicted at pH levels of 5.75 and 7.45 (Fig. 8).

3.6. Vulnerability to degradation by heavy metal mobility

The issue of metal toxicity is intricate, as the behaviour of metals is affected by various factors, with pH levels and soil organic matter (SOM) being particularly significant. Fig. 9 illustrates the changes in the vulnerability index with pH for nickel (Ni), copper (Cu), zinc (Zn), and cadmium (Cd).

The vulnerability index within the European context is illustrated in Fig. 10.. This analysis reveals that the spatial distribution is more complex than merely applying a pH threshold of 6 and is dependent on each metal as one would expect. However, since the pH = 6 has been used extensively to define metal vulnerability we also produced a European spatial distribution of soils with pH higher and lower than 6 (Fig. 11).

4. Discussion

4.1. Biochemical processes and pH thresholds

Soil pH influences biochemical processes like nutrient availability, microbial activity, plant development, and the overall health of ecosystems (Neina, 2019). Additionally, soil pH affects the solubility of minerals, which can lead to either deficiencies or toxicities depending on the pH range. Table 6 presents key pH values and ranges for various soil processes considered in this work. It is evident from Table 1 that a pH range of 5.5–7.5 is the least limiting for crop production. It is essential to acknowledge that there are numerous specialized plants that exist beyond this range and necessitate pH levels outside of this range in order to flourish. A considerable percentage of soils globally (Slessarev et al., 2016) do not fall within this least limiting range, highlighting, often a need for intervention for major crop production, ensuring cropland soils offer appropriate conditions for food production. At pH values below 5.5 toxicity can have an abrupt effect on yield reduction of many crops (Page et al., 2021). However, at pH values above 7.5 effects are more nuanced. Direct toxicity can occur due to HCO3 (Islam, 1980) and is highly species dependent, but more commonly nutrient deficiencies occur (Msimbira, and Smith, 2020), with varying impacts, such that no single threshold is easily apparent; however, it becomes increasingly likely on these marginal soils that management interventions will be required to maintain yield for food production. This scenario

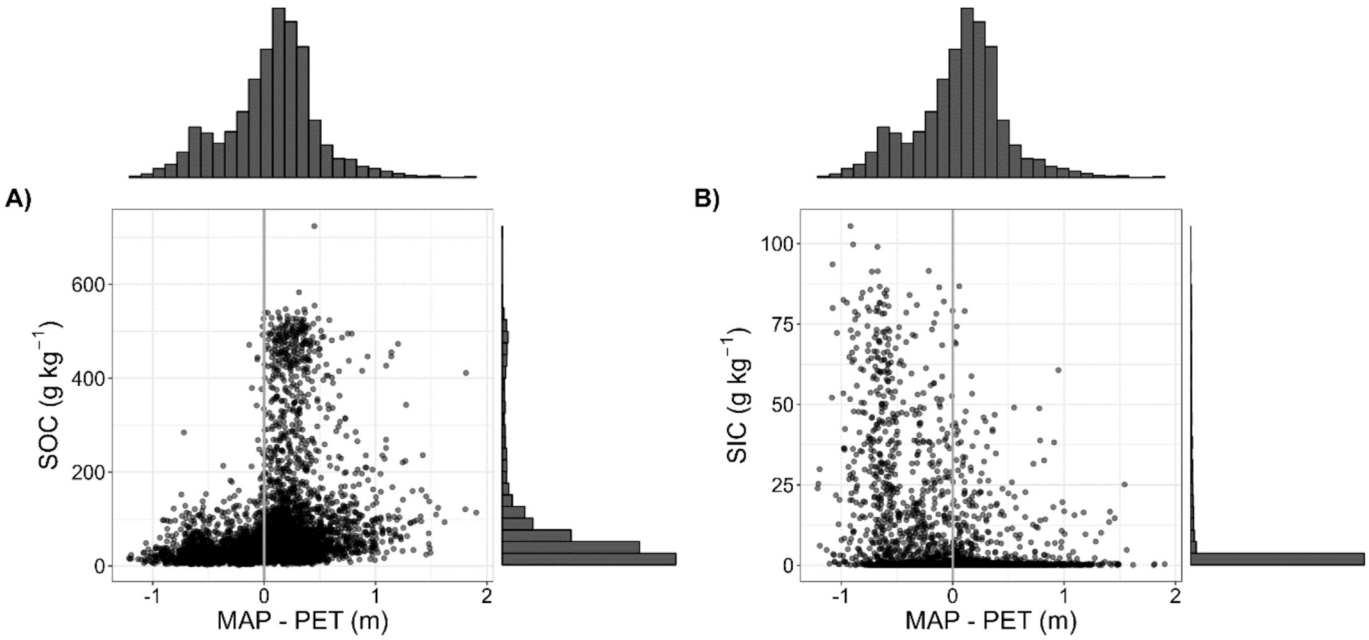

Fig. 5. A) Soil organic carbon (SOC) within the top 0–20 cm versus annual water balance (MAP-PET) for seminatural habitats ((woodlands, grasslands, shrublands and wetlands). Side panels show histograms of MAP minus PET and SOC concentrations. B) Soil inorganic carbon (SIC) versus annual water balance for semi-natural habitats.

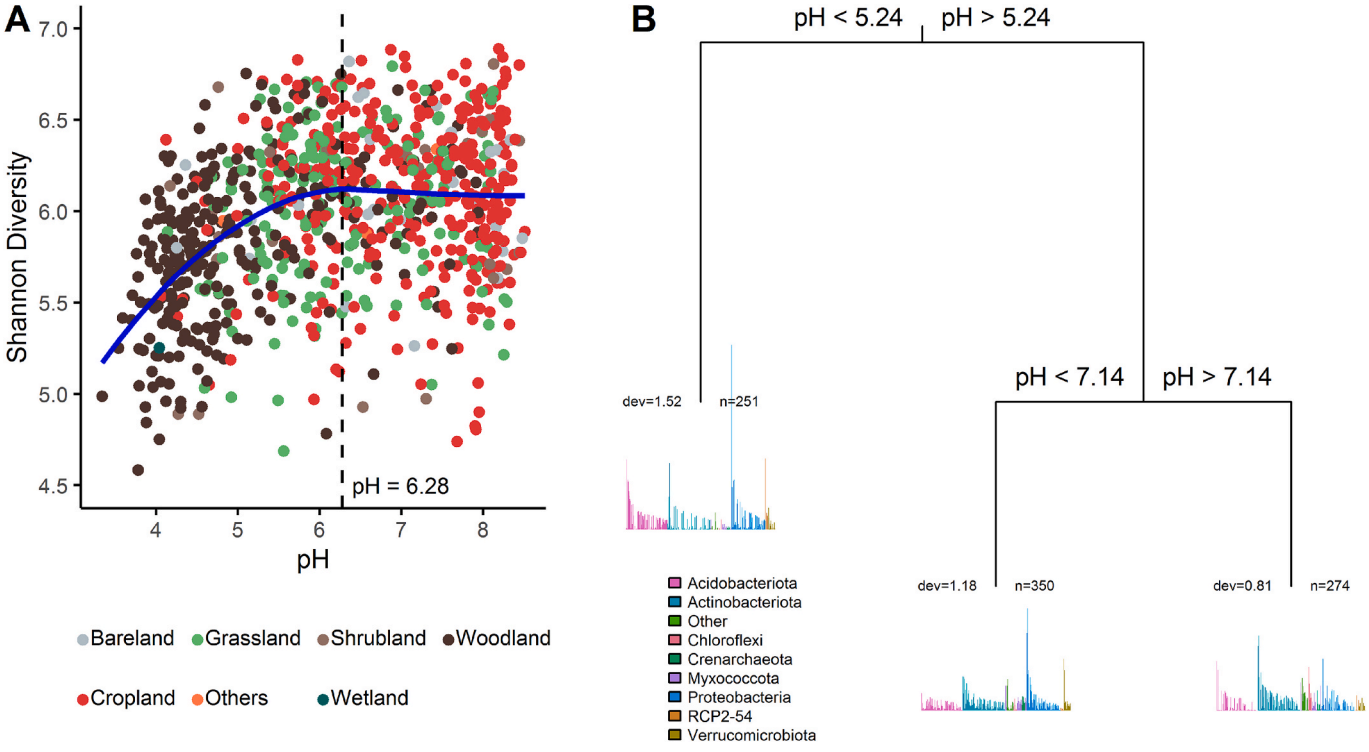

Fig. 6. A) Shannon's diversity index versus pH measured measured for European topsoils (0–20 cm). Land use information is shown as colour coded. The dashed line represents the optimum for Shannon's diversity, which is achieved at pH = 6.3. B) Multivariate regression tree identifying consistent pH defined bacterial communities with break points at pH 5.2 and ~ 7.1 spanning the diverse soils across Europe.

emphasizes the necessity for soil modification and management considering a rising population, especially as the quest for food security drives agricultural practices to encroach upon more marginal soils. Moreover, the challenge of connecting biogeochemical processes observed at the field scale to soil pH on a continental scale tends to oversimplify the complexity of the involved processes; this may be one of the limitations of the current study. In the subsequent section, we will examine the interactive influence of the water balance (MAP-PET) in conjunction with soil biochemistry within the European context, aiming to comprehend the data and identify patterns for analyzing soil health at the continental level.

Table 4
Generalized additive models (GAM) tested; using the sWorm database for European countries where site Abundance and pH values were available for the three land uses croplands, grasslands and woodlands. Data on timings of sampling (Month when the sampling had finished), extraction method and the country the data came from all added to the deviance explained in the model. The degrees of freedom (df) and the Akaike information criteria (AIC) criterion are shown. The best model was b5 which was used to predict earthworm abundance across the pH gradient and the three land uses.

Model	Model structure	Deviance explained	df / AIC
b0	Abundance ~ s(PH, k = 10)	8.3 %	10.0 / 15,869
b1	Abundance ~ s(PH, k = 10, by = Land Use)	13.8 %	15.4 / 15,807
b2	b1 + Month	20.0 %	27.2 / 15,743
b3	b1 + Month + Extraction Method	30.3 %	29.4 / 15,584
b4	b1 + Month + Country	40.6 %	43.2 / 15,423
b5	b1 + Month + Country + Extraction Method	41.5 %	45.3 / 15,410

Table 5
GAM of predicted earthworm abundance using the sWorm database (Phillips et al., 2021) using model b5 in Supplementary table tt. N = 1180, Deviance explained = 41.5 %.

Term	*edf*	*Ref.df*	*F-statistic*	*p-value*
s(pH):Cropland	*5.439*	*6.383*	*5.409*	*<0.001*
s(pH):Grassland	*2.589*	*3.240*	*2.526*	*0.0515*
s(pH):Woodland	*1.005*	*1.010*	*22.066*	*<0.001*

4.2. Water balance and the geochemical nature of soil pH

Global and continental trends indicate that environmental factors significantly influence soil pH, especially concerning the water balance. Research by Slessarev et al. (2016) has highlighted a worldwide transition from alkaline to acidic soils at the point where MAP exceeds PET in subsoils (50 cm), as subsoils are expected to be less susceptible to management pressure. The study found a bimodal distribution of soil pH, with notable peaks at pH 5.1 and pH 8.2, which align with the stability points of gibbsite and calcite, respectively. In scenarios where PET is greater than MAP, calcium tends to accumulate and form calcite; in contrast, when MAP surpasses PET, leaching occurs, resulting in aluminium becoming the dominant cation. The chemical equations that depict the shift from alkaline to acidic soils are presented in the supplementary information. The importance of the findings by Slessarev et al. (2016) is their capacity to identify soils that are less buffered and potentially more vulnerable to significant alterations.

Fig. 2A presents the distribution of pH values in European topsoils in relation to the water balance, demonstrating that these topsoils do not follow a distinct bimodal distribution pattern. While it is conceivable that there is a notable concentration of soils with a pH near 6.5 in Europe, it is more likely that the pH variations observed in the dataset stem from uniform agricultural practices and management strategies, such as the use of lime and organic amendments. When cropland and livestock pasture areas were removed from the dataset, a bimodal distribution emerged, as shown in Fig. 2B, consistent with Slessarev et al. (2016).

The optimal pH range for most crop production is identified as 6–7 (Vitousek et al., 2004, Roy et al., 2006). Consequently, it is not unexpected that the removal of croplands and livestock pastures, as illustrated in Fig. 2A, reveals a distribution where numerous soils within the 6–7 pH range have been lost (Fig. 2B). This suggests that anthropogenic inputs maintain soils out of the natural equilibrium for biomass production. Given the implications of climate change, this scenario raises concerns about the sustainability of certain agricultural methods, especially those that deviate further from equilibrium, as they will necessitate greater inputs to maintain pH levels conducive to productivity or may require a shift to different crop varieties.

Fig. 2B illustrates that the bimodal distribution observed in European soils does not exhibit peaks at 8.2 and 5.1, as seen in the global soils

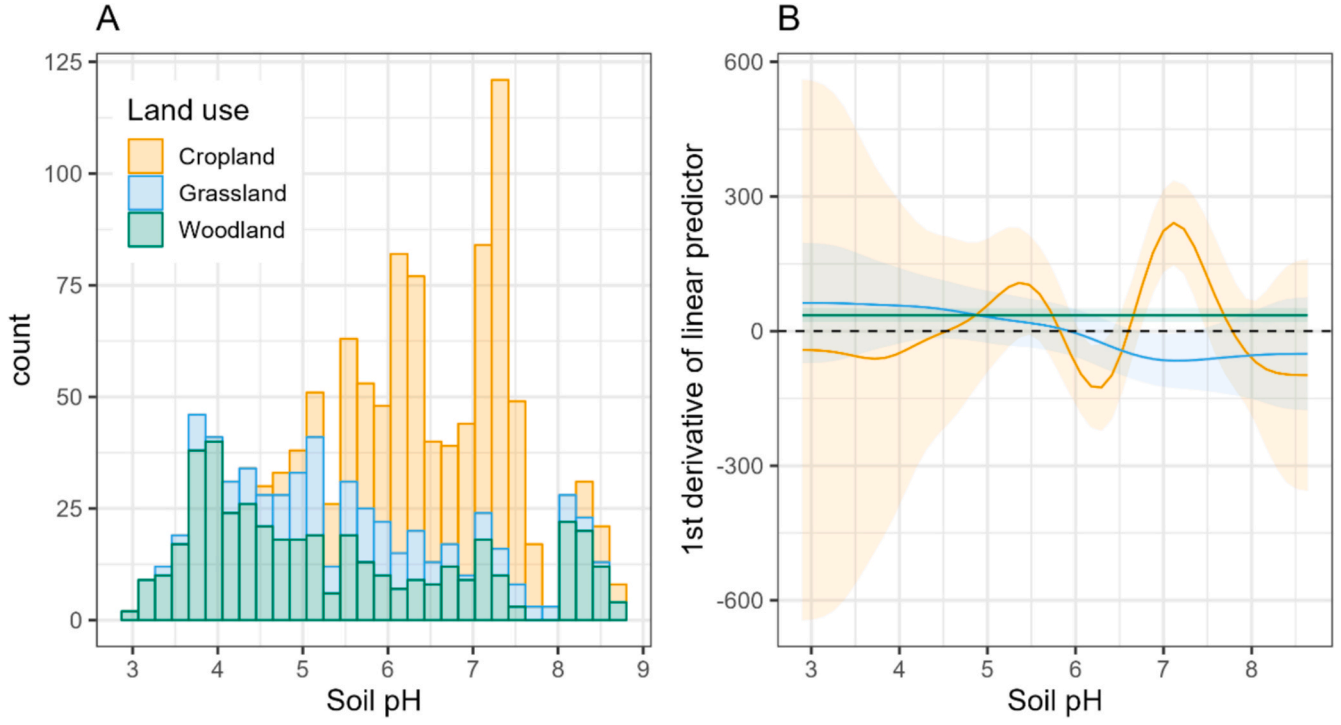

Fig. 7. A) Histogram of the number of pH measurements by land use. B) First derivative of the linear predictor in relation to Fig. 7A, derived for predicted earthworm abundances across the soil pH range for European croplands, grasslands and woodlands.

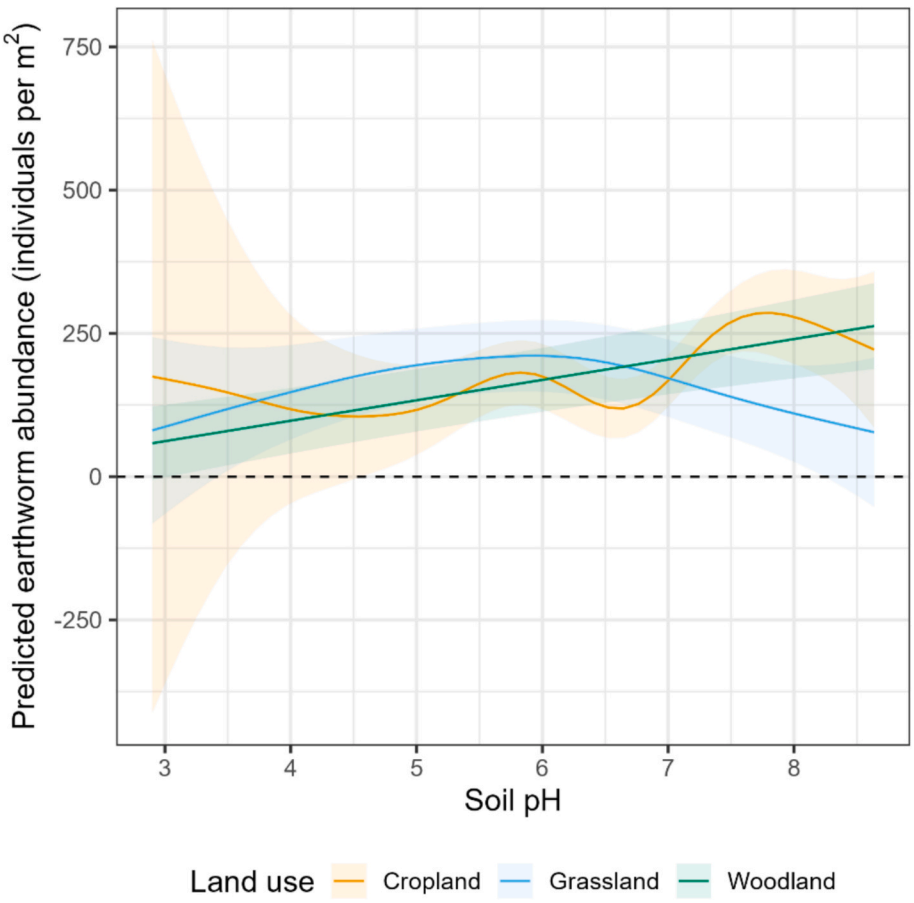

Fig. 8. Predicted earthworm abundance and 95% confidence interval across the pH range for croplands, grasslands and woodlands. European data from the global sWorm database from (Phillips et al., 2021).

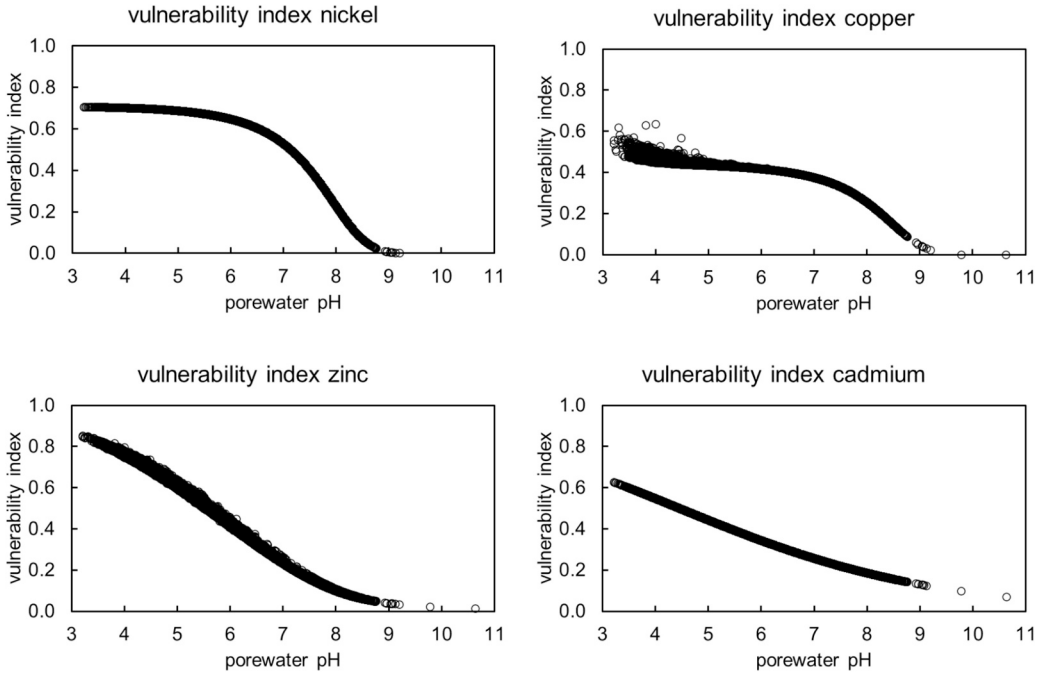

Fig. 9. Computed vulnerability indices for nickel, copper, zinc and cadmium in LUCAS soils as a function of the porewater pH.

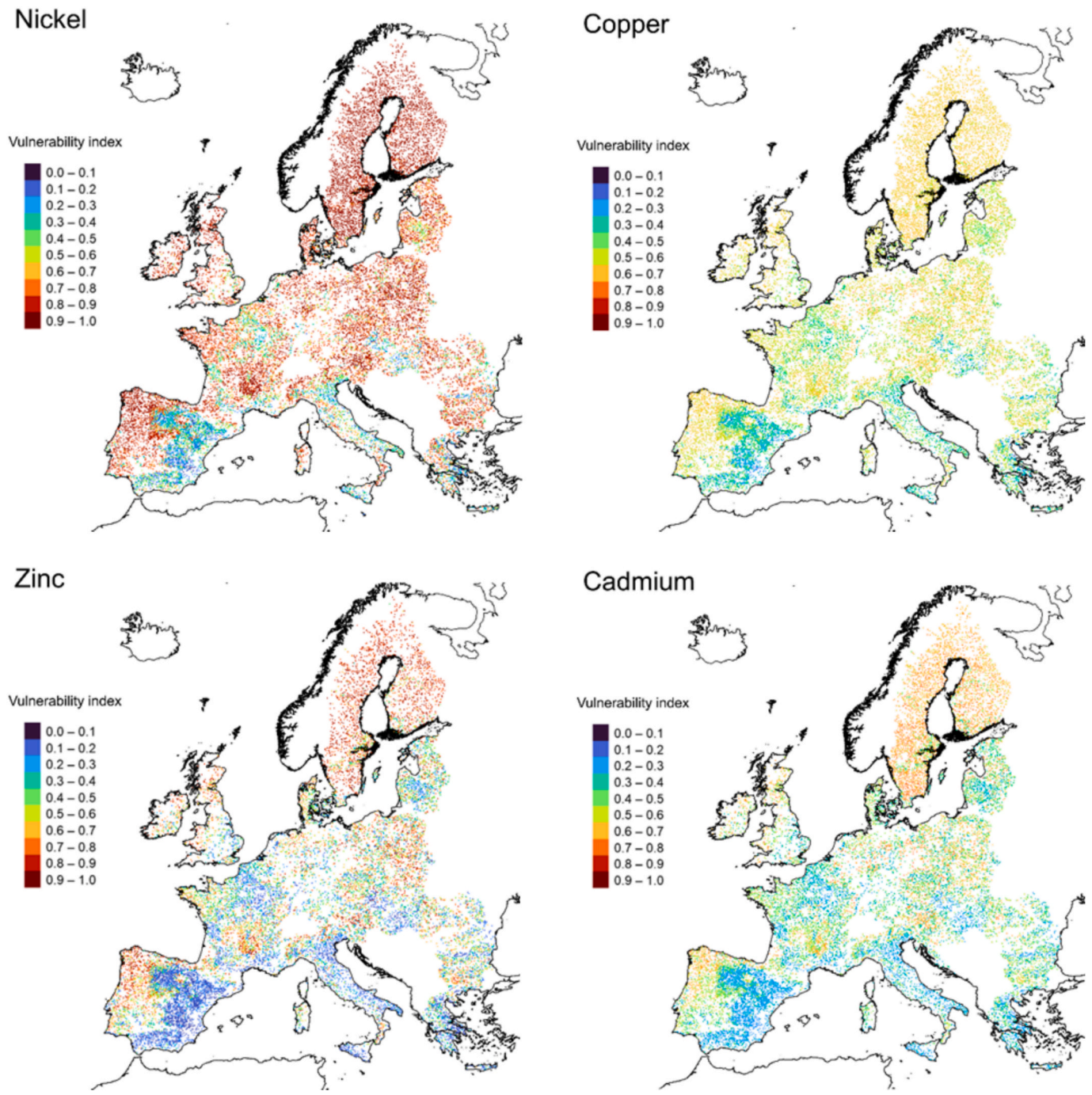

Fig. 10. Mapped vulnerability indices for nickel, copper, zinc and cadmium mobility according to LUCAS 2018 topsoil (0–20 cm) data.

analysed by Slessarev et al. (2016). Instead, these peaks are shifted towards lower values, suggesting that European soils have undergone partial leaching, which contributes to a trend of acidification (refer to Appendix D). Ecosystems can progress beyond the equilibrium states of calcite and gibbsite, leading to more severe conditions that may compromise soil health and its ability to sustain life. For example, when MAP exceeds PET, the soil's water content is affected not only by the influx of water but also by the soil's hydraulic characteristics. Factors such as soil texture, structure, organic matter levels, compaction, and the depth of the water table play crucial roles in determining the duration that water remains within the soil. The alternating cycles of wetting (reduction) and drying (oxidation) trigger redox reactions that facilitate the transfer of electrons among various chemical species, potentially altering the pH by as much as 2 units (Thompson et al., 2006). Significant redox processes in soils, which involve minerals such as iron and manganese oxides, are elaborated in the supplementary material and have important consequences for microbial activity, nutrient availability, weathering rates, and the mineral composition of the soil system.

The geographical distribution of soils with pH levels below 5.1 and above 8.2 across Europe is depicted in Fig. 3. This illustration emphasizes the influence of the water balance on the leaching or accumulation of salts within the soil. Soils with pH levels below 5.1 are typically found in regions with a Nordic climate, characterized by cold winters and mild, humid summers, as well as in areas with an oceanic climate, which features mild winters and humid summers in Western Europe.

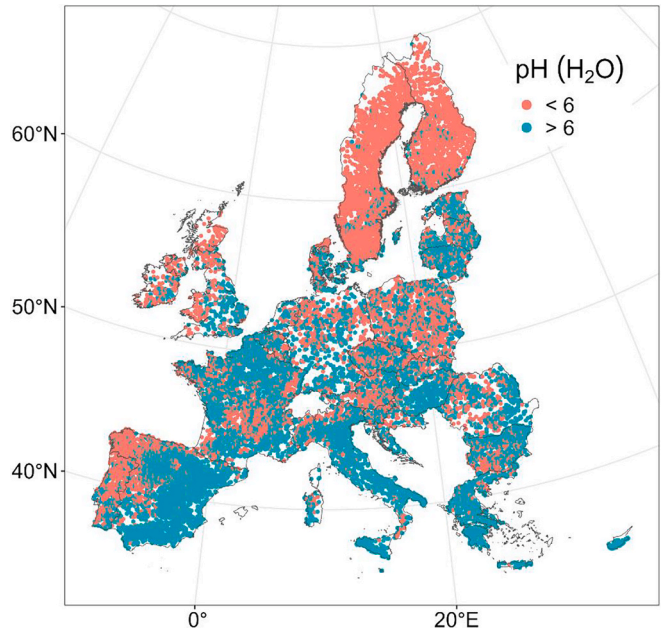

Fig. 11. Spatial distribution of soils in Europe with a pH value less than 6, in red.

Conversely, Southern European countries, which experience a Mediterranean climate, predominantly contain soils with pH levels close to, or exceeding, 8.2. Although the prevalence of soils with pH levels above 8.2 is relatively low in Europe, their economic significance warrants attention, as they are generally situated in highly productive agricultural regions, such as the Ebro Basin in Spain. These soils have been the subject of extensive research due to their susceptibility to desertification, a process that often begins with soil alkalinization. The combination of elevated pH, that affects the charge balance for variable charge sites on minerals and organic matter, and sodium presence can adversely affect soil characteristics, leading to issues such as colloid dispersion, SOC loss, reduced soil permeability, and increased runoff and erosion (Allison and Richards, 1954; Lebron et al., 1994). This process is initiated by water movement, which facilitates the transport of dispersed colloids that clog soil pores, resulting in densification and diminished hydraulic conductivity. Once the soil structure is compromised, restoration can be exceedingly challenging. The mechanisms responsible for the high pH values observed in soils are detailed in the supplementary information.

4.3. Topsoil carbon

Climate has long been recognized as a key factor influencing SOC levels (Carvalhais et al., 2014). However, recent studies indicate that climate, moisture, and geochemical factors interact significantly in the mechanisms of soil carbon storage (Doetterl et al., 2015; Yu et al., 2021). Soil pH serves as a valuable indicator of the geochemical processes occurring within the soil. Fig. 4 illustrates the correlation between SOC and pH across European soils, alongside the relationship between SIC and pH. As pH approaches neutral and alkaline ranges, there is an increase in the dissociation of functional groups within SOM (Andersson et al., 2000), and the bonds at the mineral interface between clay minerals and organic compounds weaken (Curtin et al., 1998). These concurrent phenomena lead to enhanced dissolution and transport of SOM (Neina, 2019). Fig. 4 demonstrates that the soil's capacity to retain SOM diminishes as pH rises towards more alkaline levels, with a notable overlap occurring around pH 7.2, where SIC begins to accumulate more rapidly as pH continues to increase. Exceptions to this pattern include fenland soils, which have an alkaline pH but maintain carbon through high productivity and oxygen limiting conditions suppressing decomposition that allows for SOC accumulation even when adjacent waters have a pH above 7. Additionally, certain low pH soils can be found over calcareous parent materials, showing that with sufficient time, climate and biological factors become dominant at driving pH in topsoil. Despite these anomalies, a clear general trend is evident: as pH rises, SOC decreases, and SIC levels increase beyond pH 7.2, with SIC becoming the dominant form of carbon, in line with pedological theory (Jenny, 1994). It is expected that calcite will be the main form of SIC within the pH range of 7 to 9 (van Breemen et al., 1983), although other carbonates may gain prominence at pH levels above 8.1; however, such high pH soils are primarily confined to the southern regions of Europe. The transition from SOC to SIC is often linked to a decrease in moisture

Table 6
Synthesis of key pH values and ranges for biogeochemical processes and plant growth from the literature. This table serves as a guide only and values are not universal definitive thresholds. CUE = Carbon Use Efficiency, SOM = Soil Organic Matter.

Process	pH	Effect outside the pH range	Reference
acid phosphorus enzyme activity	4–5	Limited phosphorus availability	(Turner and Romero, 2010)
Fungal activity	4–6	Reduced activity	(Neina, 2019)
Bioturbation by earthworm activity	5–7	less bioturbation and distribution of SOM, reduced soil connectivity, Different by land use	(Hakonen et al., 2010) present study
Al dissolution	<5.1	Plant growth limitations, forest die back etc	(Lofts, 2022)
Iron dissolution	<5.5	toxicity in the acid range	(Lofts, 2022)
Crop yield decline due to toxicity	<5.5	Many common crops suffer significant (50 %) relative yield declines. (species dependent)	(Rowell, 1988; Page et al., 2021)
Heavy metals dissolution	<6–7	More toxicity	(Lofts, 2022)
Microbial carbon use (CUE) efficiency	6.2	Below 6.2 CUE goes to zero	(Malik et al., 2018)
Microbial activity	6–7.5	Reduced bacterial activity	(Labouyrie et al., 2023)
Organic matter decomposition	6–7	Slower decomposition	(Malik et al., 2018)
Priming of SOM	5.5–7.5	Slower decomposition	(Wang and Kuzyakov, 2024)
Plant growth least limiting range	5.5–7.5	Increasing constraints	Roy et al., 2006; Msimbira and Smith (2020); (Vitousek et al., 2004);
Microbial diversity	>6.28	Reduced diversity	(Griffiths et al., 2011); Seaton et al. (2024) Present study
Transition between organic dominated to inorganic carbon dominated	~7	Has implications for carbon accumulation and storage	Present study
Plant growth nutrient deficiency	>7.5	Species dependent growth affected by excess HCO_3 or potential deficiency of Fe, P and Zn or imbalance of Ca, Mg and K.	Islam, (1980); Msimbira and Smith (2020)
Calcite buffering	8.2	Drastic changes of pH affecting biogeochemical reactions in soils	(Van Breemen et al., 1983)
Sodification	>9	Often associated with soil salinity and structural deterioration	(Lebron et al., 1994)
alkaline phosphorus enzyme activity	10–11	Limited phosphorus availability	(Turner and Romero, 2010)

content, which aligns with the data presented in Fig. 4 and the annual water balance (MAP-PET).

It is essential to assess pH within the framework of environmental variables, such as climatic conditions and parent material. Fig. 5 illustrates that SOC can only build up to more than 200 g/Kg in soils when MAP exceeds PET; conversely, when PET surpasses MAP, conditions become more conducive to the accumulation of SIC. The data presented in Fig. 5 highlight a significant interplay between geochemical factors and climate in determining a soil's capacity to sequester carbon, this observation has also been made by Hansen et al. (2024). We focused on seminatural habitats for the plots in Fig. 5 to eliminate the influence of human activity. It is crucial to note that SOC can accumulate in soils with either high or low pH, provided they are moist; however, it does not accumulate in dry, high pH soils. This observation may suggest that moisture levels are a more critical factor than pH in inhibiting microbial turnover or oxidation processes.

4.4. Health and microbial response to pH

Advancements in DNA and metagenomic technologies have provided insights into the previously uncharted soil microbiome. Investigations into the microbiome, particularly its diversity, have revealed relationships between bacterial diversity and soil pH levels. Soil pH is recognized as a significant factor influencing soil microbial communities, with numerous global studies indicating that pH serves as the foremost predictor of bacterial communities across extensive environmental gradients, which encompass a variety of climatic conditions and land uses (Bahram et al., 2018; Fierer and Jackson, 2006; Griffiths et al., 2011; Labouyrie et al., 2023). These associations are often established by comparing environmental characteristics with either univariate metrics derived from sequencing data, such as taxonomically agnostic richness estimates, or through multivariate ordination techniques that provide deeper insights into compositional changes. Typically, bacterial diversity exhibits either positive or humped relationships with pH (Fig. 6A), this pattern aligns with the results of previous studies, such as those by Fierer and Jackson (2006), which identified a similar optimal pH. Additionally, data from temperate experimental sites suggest that when pH falls below 6.2, microbial carbon use efficiency (CUE) significantly decreases, which has important implications for carbon processing (Malik et al., 2018). Ordination methods reveal distinct community assemblages along pH gradients, highlighting the ecological responses of specific taxa to variations in pH (Jones et al., 2021; Zhou et al., 2024). In their study utilizing multivariate regression trees to analyse compositional and abundance changes across various British soils, Griffiths et al. (2011) identified critical transition points within bacterial communities that corresponded to shifts in land use and pH. The primary division in the dataset was influenced by land use, distinguishing typically acidic environments, such as bogs, moors, and upland woods, from arable lands, grasslands, and lowland woods. Within these divisions, a clear distinction based on pH emerged, with acidic habitats categorized into two groups above and below pH 5.2, while non-acidic habitats were similarly divided above and below pH 6.9.

We examined comparable data from the EU-wide LUCAS survey, which also identified similar pH breakpoints of 5.2 and 7.1 delineating three broad community types across a range of soil types (Fig. 6B) It suggests that the soil bacterial communities can be considered to split into acidophiles, neutrophiles and alkaliphiles between these thresholds. It is important to note that different sequencing techniques were employed in the LUCAS survey, including the use of various primers. More significantly, the EU survey encompassed a variety of habitats, specifically targeting arable, grassland, and wooded communities, while excluding the typically carbon-rich upland moor and bog habitats that were appropriately sampled with the stratified random design in the GB survey (Robinson et al., 2024). Collectively, these findings underscore the critical role of soil pH as a primary factor influencing the composition of dominant bacterial taxa, often surpassing the impact of related land use variables, thereby highlighting the widespread significance of pH. Furthermore, additional breakpoints around pH 5 and 7 have been observed in the assessment of archaeal communities, as noted by Gubry-Rangin et al. (2011) and Seaton et al. (2024).

4.5. Earthworms and soil health

Soil pH is also linked to earthworm species composition and overall abundance. In strongly acidic soils, pH < 3, fewer tolerant taxa tend to dominate diversity, but their abundances are generally low. In woodlands, this is particularly evident from studies comparing earthworms under different tree species, with changes in earthworm abundance related to differences in the quality of litter inputs and associated changes in litter layer accumulation, soil biogeochemistry and pH e.g. (Neirynck et al., 2000; Reich et al., 2005; Schelfhout et al., 2017). Such changes hinge on the pH threshold at $\sim$ 4.5 separating soil processes dominated by aluminium/iron and base cation exchange, and a vertical decoupling of litter incorporation, with many earthworm species being intolerant at lower soil pH. The study by Desie et al. (2019) demonstrated the overriding importance of tree inputs at lower soil pH, relative to inherent differences in exchange domain, with conversion from deciduous to coniferous species enacting reductions in pH and lower earthworm abundance and biomass. In a common garden experiment of 14 tree species, Reich et al. (2005) found positive relationships between litter calcium, exchangeable calcium in soil and earthworm biomass. Where tree species with rich litter are found on alkaline parent material or soils, exceptionally high earthworm abundance can be found (Lakhani and Satchell, 1970; Piearce, 1972). The linear increase in predicted earthworm abundance with soil pH for woodlands presented in our study may represent these mechanisms, playing out at the European scale.

The unimodal relationship between predicted earthworm abundance and soil pH in grassland, with a pH optimum just below 6, combines effects of pH, management and climate. Previous studies of temperate grasslands have found greater earthworm abundances to be linked to higher pH (Hoeffner et al., 2021). Indeed, greater earthworm abundance have been found following the liming of acidic grasslands and associated increases in soil pH (McCallum et al., 2016). The decline in predicted earthworm abundance at higher pH for grasslands likely reflects a predominance of higher pH representing locations with drier climate and associated reductions in SOC. In croplands, tillage is a critical factor impacting earthworm abundance (Briones and Schmidt, 2017) and management may be the primary driver of earthworm abundance e.g. (Frazão et al., 2017). The bimodal peaks in predicted earthworm abundance for croplands presented in this study likely represent agricultural management which optimises conditions for earthworms under different soil types or geographies.

4.6. Soil degradation through metals

One of the major potential challenges to food security in Europe is the contamination caused by metals that are released from pollution or environmental sources, particularly heavy metals. The presence of heavy metals often stems from the historical activities of various industries, including agricultural practices. The solubility and bioavailability of numerous heavy metals are significantly affected by pH levels, with critical thresholds that influence their movement. A review of the current literature indicates that a pH level below 6 is widely acknowledged as a threshold at which the mobility of heavy metals increases the associated risks (Król et al., 2020). The distribution of soils with a pH lower than 6 is illustrated in Fig. 11, revealing that most regions in Europe, except for parts of Spain, Italy, Croatia, and Greece that have more calcareous soils, are vulnerable to metal mobility.

pH serves as a crucial indicator of metal solubility, with geochemical thresholds of 5.1 and 8.2 playing a significant role in determining metal

abundance and toxicity. Soils with a pH below 5.1 (see Fig. 3A) are prone to the dissolution of aluminium, primarily in the form of Al^{3+}, which is harmful to plant roots and has been linked to forest dieback caused by acid rain across Europe. The presence of Al^{3+} interferes with root cell division and elongation, resulting in stunted root development and a decrease in fine root hairs. This impairment limits the plant's ability to absorb water and nutrients, causing drought stress even when water is present. Furthermore, $Al3^{+}$ competes with vital cations such as Ca^{2+}, Mg^{2+}, and K^{+}, diminishing their availability. It also reacts with phosphate ions to create insoluble $AlPO_4$, rendering phosphorus inaccessible to plants. Additionally, aluminium toxicity adversely impacts microbial communities that are essential for nutrient cycling and the decomposition of organic matter, as illustrated in Fig. 6A, which shows a decline in microbial diversity. Al^{3+} is detrimental to numerous beneficial bacteria and fungi, leading to a reduction in microbial populations, particularly affecting nitrogen-fixing bacteria (Rhizobia) and consequently hindering symbiotic nitrogen fixation in legumes.

Elevated pH levels exceeding 8.2 can lead to complications concerning metal ions, as the solubility of various metal cations, such as iron (Fe), zinc (Zn), copper (Cu), manganese (Mn), aluminium (Al), lead (Pb), and cadmium (Cd), diminishes due to the formation of insoluble compounds like hydroxides and carbonates. Nonetheless, some metals may remain dissolved, influenced by their specific chemical forms and their interactions with soil constituents. For instance, oxyanions such as arsenic (As) in the form of arsenate (AsO_4^{3-}), selenium (Se) as selenate (SeO_4^{2-}), and boron (B) as borate ($B(OH)_4^{-}$) can exhibit increased solubility under alkaline conditions. Sodium is another element that demonstrates high solubility and has a complex relationship with pH levels. In non-saline sodic soils, sodium displaces calcium (Ca^{2+}) and magnesium (Mg^{2+}) from soil particles, which results in the dispersion of clay and organic matter. This process diminishes the soil's buffering capacity and leads to the accumulation of carbonates (CO_3^{2-}) and bicarbonates (HCO_3^{-}), consequently elevating soil pH; in some sodic soils, pH values may surpass 9. Although infrequent, in acidic soils, sodium can interact with aluminium (Al^{3+}), resulting in acidification. The presence of sodium poses challenges not only to plant growth by increasing osmotic potential but also contributes to structural degradation through the dispersion of clay particles, as previously mentioned.

Heavy metal leaching in soils is primarily influenced by pH levels and soil organic matter (SOM) (Lofts, 2022; van der Sloot and van Zomeren, 2012). Even minor changes in pH can result in fluctuations in metal concentrations due to various processes, including dissolution/precipitation, adsorption/desorption on mineral and organic substrates, and complexation with ligands in the solution (Lofts, 2022). We evaluated the vulnerability index for Ni, Cu, Zn, and Cd concerning pH levels in European soils (Fig. 9). A significant pH threshold was observed for Ni and Cu around pH 7, beyond which their vulnerability sharply declined. Conversely, the reduction in vulnerability for Zn and Cd was more gradual, although it still decreased with increasing pH. When this vulnerability index was mapped across Europe (Fig. 10), the geographical distribution closely mirrored the pH maps shown in Fig. 11, indicating that countries with acidic pH values are more susceptible to metal toxicity. The vulnerability varies by metal, with Ni exhibiting a higher tendency to leach in areas where pH is below 6. Tóth et al. (2016) report that Ni concentrations in Europe are generally low, at under 25 mg/Kg; nonetheless, the vulnerability remains significant. In regions where pH exceeds 6, the overall vulnerability markedly diminishes. The presence of elevated levels of heavy metals in soil solutions adversely affects primary productivity, which in turn restricts carbon inputs into the soil and limits carbon storage under these conditions (Yu et al., 2021).

4.7. Modelling climate driven pH changes and future work

The rate of biogeochemical changes in soil can vary, occurring either gradually or rapidly, depending on the internal chemical reactions to environmental influences. Climate change forecasts for Europe suggest modifications in the frequency and intensity of rainfall, with an increased probability of extreme weather events during both winter and summer (Stocker, 2015). These shifts result in more frequent occurrences of intense, short-lived rainfall followed by extended periods of drought (Chan et al., 2014; Hirabayashi and Kanae, 2009; Kharin et al., 2007; Kundzewicz et al., 2014). The alternating cycles of wetting and drying serve as significant factors driving the spatial and temporal variability in soil characteristics, which in turn impact the biogeochemical processes occurring within the soil (Robinson et al., 2019; Schulz-Zunkel et al., 2015; Tockner et al., 2010). Such changes encompass fluctuations in redox potential, which subsequently affect the concentrations of iron (Fe) and manganese (Mn), ultimately influencing soil pH levels (Rinklebe and Shaheen, 2017).

Assessing the influence of climate variability, trends, and extremes on soil pH necessitates a modelling framework that encompasses environmental, geochemical, and biological processes. These processes can be effectively integrated into modelling frameworks via the calibration of process-based models, the application of statistical and artificial intelligence (AI)-based models, and the creation of hybrid approaches that merge both methodologies. Process-based models, such as MAGIC (Cosby et al., 2001), VSD+ (Bonten et al., 2016), and ForSAFE (Wallman et al., 2005), predict soil pH by combining climate variables—such as temperature, precipitation, and CO_2 concentrations—with soil chemistry, hydrology, and biological interactions over time. AI-driven models leverage statistical and machine learning methods to uncover predictive relationships between environmental variables and soil pH, utilizing historical and spatially distributed datasets (Were et al., 2015). Conversely, hybrid methodologies take advantage of the mechanistic insights offered by process-based models while integrating AI to improve predictive accuracy through data fusion techniques (Afshar et al., 2019).

Process-based models provide a mechanistic framework for simulating changes in soil pH across various environmental contexts. These models account for time-dependent processes such as acidification, buffering, and leaching, allowing them to capture the long-term dynamics of soil pH (Zeng et al., 2017). However, they require calibration specific to individual sites, utilizing time series data obtained from field measurements, which makes them computationally intensive and applicable only to certain areas (Reinds et al., 2008). Additionally, although these models excel at simulating gradual climate changes, they may struggle to accurately depict nonlinear and unforeseen extreme events due to their dependence on established relationships, which might not sufficiently represent the conditions brought about by climate extremes (Holmberg et al., 2018).

Statistical and AI-based approaches can effectively handle the complex relationships between climate and soil pH by utilizing spatially distributed datasets (Xiao et al., 2023). A notable advantage of AI models is their ability to incorporate a diverse range of spatial observations, especially in cases where temporal data is limited (Borrelli et al., 2020; Hassani et al., 2021). However, the performance of these models may be limited by uneven data distribution or biases that exist within the training dataset.

Hybrid methodologies tackle these issues by integrating process-oriented mechanistic insights with AI-driven pattern recognition (Jin et al., 2018). While AI-based models consider predictions as isolated instances, process-based models consider the historical factors influencing soil pH (Zhao et al., 2019). Soil acidification or alkalization may stem from the cumulative effects of climate over several years or even decades, rather than merely from short-term environmental changes (Rengel, 2011). Hybrid modelling strategies that employ data assimilation techniques can improve the predictive precision of soil pH assessments, ensuring that both the temporal continuity of soil processes and the spatial variability of environmental conditions are adequately represented.

These modelling frameworks can be adapted to predict future soil pH

changes under various climate change scenarios. By calibrating process-based models to replicate long-term soil responses or training artificial intelligence models on historical correlations among climate variables, land use, and soil pH, these frameworks can generate soil pH forecasts using climate data from Earth system models, including those from the Coupled Model Intercomparison Project (CMIP). The inclusion of climate projections derived from different Shared Socioeconomic Pathways (SSPs) facilitates scenario-based evaluations of soil pH changes in the future. This integration provides a more thorough understanding of potential trends in soil acidification or alkalization, assisting land managers and policymakers in formulating adaptive soil management strategies considering anticipated climate conditions.

It is essential to begin forecasting pH variations in soils throughout Europe, and more widely the globe, to anticipate alterations resulting from climate change, land use, or land management practices. Recognizing areas at high risk will provide policymakers with the necessary foresight to minimise or avert soil degradation.

5. Conclusions

The examination of topsoil pH trends throughout Europe, as recorded by LUCAS, indicates that seminatural habitats exhibit a bimodal distribution of topsoil pH values. In contrast to global soils, which peak at pH values of 5.1 and 8.2, European topsoils are skewed towards lower pH values (4.41 and 7.54). This shift suggests that European soils have undergone partial leaching, contributing to a trend of acidification. As a result, there is increased susceptibility to metal and heavy metal leaching vulnerability across European soils in compared to their global counterparts. Furthermore, our findings indicate that human activities, such as food production and associated land management, are displacing soils from their natural equilibrium, particularly towards the pH range of 6–7. Considering climate change, this situation raises serious concerns regarding the sustainability of specific agricultural practices, especially those that further deviate from equilibrium, as they will require increased inputs to sustain pH levels that are favourable for productivity.

A consistent trend is discerned and significant thresholds for utilizing pH as a measure of soil health and degradation in the context of environmental changes across Europe. Notably, a pivotal transition occurs at pH 7.2, where soil organic matter (SOM) diminishes in favour of the accumulation of soil inorganic carbon (SIC). This transition has been associated with climatic factors, indicating that a mean annual precipitation minus potential evapotranspiration (MAP-PET) greater than zero is necessary for SOM accumulation, while conditions where MAP-PET is less than zero favour calcite deposition in the soil. Regarding soil health, the application of multivariate regression trees has enabled us to illustrate the significance of soil pH as a key factor affecting the dominant taxa. This classification highlights three general community types across different soil types, acidophiles, neutrophiles and alkaliphiles between these thresholds further establishing pH as the most dependable predictor for soil microbial populations. Patterns for earthworms were more nuanced generally with more distinct optima based on land use. Regarding vulnerability and degradation, soil moisture content and subsequently pH have been shown to influence the susceptibility to metal toxicity, particularly nickel. Nickel is prone to leaching in regions where soil pH falls below 6, particularly in humid climates. It is crucial to initiate predictions of pH fluctuations in soils throughout Europe to prepare for changes induced by climate change, land use, or land management practices. Identifying regions at elevated risk will equip policymakers with the foresight needed to minimise or prevent soil degradation.

Author Contributions Statement

IL & DAR handled the conceptualization and writing of the original draft with CF providing the climate component; SR, KS, IL and DAR the carbon component RG, DF, BJ writing the microbial component, AK and SR contributed the earthworm component; SL contributed the metals component, and NS, MA the modelling and future work section. All contributed to review & editing. DAR handled the funding acquisition.

During the preparation of this work the authors used ahrefs sentence rewriting tool in order to improve the consistency of the language across multiple international authors. After using this tool, the authors reviewed and edited the content as needed and take full responsibility for the content of the publication.

CRediT authorship contribution statement

Inma Lebron: Writing – review & editing, Writing – original draft, Methodology, Investigation, Formal analysis, Conceptualization. **Christopher J. Feeney:** Writing – review & editing, Formal analysis, Data curation. **Sabine Reinsch:** Writing – review & editing, Methodology, Formal analysis. **Nima Shokri:** Writing – review & editing, Methodology, Formal analysis. **Mehdi H. Afshar:** Writing – review & editing, Methodology, Formal analysis. **Steve Lofts:** Writing – review & editing, Writing – original draft, Methodology, Formal analysis. **Rob Griffiths:** Writing – review & editing, Writing – original draft, Software, Methodology, Formal analysis. **David Fidler:** Writing – review & editing, Software, Methodology, Formal analysis. **Briony Jones:** Writing – review & editing, Formal analysis. **Panos Panagos:** Writing – review & editing, Data curation. **Kasia Sawicka:** Writing – review & editing, Formal analysis. **Aidan M. Keith:** Writing – review & editing, Formal analysis, Data curation. **Fiona Seaton:** Writing – review & editing. **David A. Robinson:** Writing – review & editing, Writing – original draft, Supervision, Project administration, Methodology, Investigation, Funding acquisition, Formal analysis, Conceptualization.

Funding

The research was funded by the.

- The Research Council of Norway, Climasoil, Project number: 325253.
- This research was supported/partially supported by NERC, through the UKCEH National Capability for UK Challenges Programme NE/Y006208/1.
- This project acknowledges funding from the European Union's Horizon Europe research and innovation program under grant agreement No.-101086179; and funding from the UK Research and Innovation (UKRI) under the UK government's Horizon Europe funding guarantee [grant number 10053484] as part of AI4SoilHealth.

Declaration of competing interest

The authors declare that they have no known competing financial interests or personal relationships that could have appeared to influence the work reported in this paper.

Acknowledgments

Disclaimer: Work funded by the European Union. Views and opinions expressed are however those of the author(s) only and do not necessarily reflect those of the European Union or the Research Executive Agency. Neither the European Union nor the granting authority can be held responsible for them.

Appendix A. Supplementary data

Supplementary data to this article can be found online at https://doi.org/10.1016/j.catena.2025.109454.

References

Afshar, M.H., Yilmaz, M.T., Crow, W.T., 2019. Impact of rescaling approaches in simple fusion of soil moisture products. Water Resour. Res. 55, 7804–7825.

Allison, L., Richards, L.A., 1954. Diagnosis and improvement of saline and alkali soils: Soil and Water Conservative Research Branch. Agricultural Research Service ….

Andersen, C.B., 2002. Understanding carbonate equilibria by measuring alkalinity in experimental and natural systems. J. Geosci. Educ. 50, 389–403.

Andersson, S., Nilsson, S.I., Saetre, P., 2000. Leaching of dissolved organic carbon (DOC) and dissolved organic nitrogen (DON) in mor humus as affected by temperature and pH. Soil Biol. Biochem. 32, 1–10.

Anthony, M.A., Bender, S.F., van der Heijden, M.G., 2023. Enumerating soil biodiversity. Proc. Natl. Acad. Sci. 120, e2304663120.

Auguie B, Antonov A. gridExtra: Miscellaneous functions for "grid" graphics (Version 2.3). R Core Team: Vienna, Austria 2017.

Bahram, M., Hildebrand, F., Forslund, S.K., Anderson, J.L., Soudzilovskaia, N.A., Bodegom, P.M., et al., 2018. Structure and function of the global topsoil microbiome. Nature 560, 233–237.

Ballabio, C., Panagos, P., Lugato, E., Huang, J.-H., Orgiazzi, A., Jones, A., et al., 2018. Copper distribution in European topsoils: an assessment based on LUCAS soil survey. Sci. Total Environ. 636, 282–298.

Ballabio, C., Jones, A., Panagos, P., 2024. Cadmium in topsoils of the European Union–an analysis based on LUCAS topsoil database. Sci. Total Environ. 912, 168710.

Bonten, L.T., Reinds, G.J., Posch, M., 2016. A model to calculate effects of atmospheric deposition on soil acidification, eutrophication and carbon sequestration. Environ. Model. Software 79, 75–84.

Borrelli, P., Robinson, D.A., Panagos, P., Lugato, E., Yang, J.E., Alewell, C., et al., 2020. Land use and climate change impacts on global soil erosion by water (2015-2070). Proc. Natl. Acad. Sci. 117, 21994–22001.

Briones, M.J.I., Schmidt, O., 2017. Conventional tillage decreases the abundance and biomass of earthworms and alters their community structure in a global meta-analysis. Glob. Chang. Biol. 23, 4396–4419.

Bünemann, E.K., Bongiorno, G., Bai, Z., Creamer, R.E., De Deyn, G., De Goede, R., et al., 2018. Soil quality–a critical review. Soil Biol. Biochem. 120, 105–125.

Callahan BJ, McMurdie PJ, Rosen MJ, Han AW, Johnson AJA, Holmes SP. DADA2: High-resolution sample inference from Illumina amplicon data. Nature methods 2016; 13: 581-583.Carvalhais N, Forkel M, Khomik M, Bellarby J, Jung M, Migliavacca M, et al. Global covariation of carbon turnover times with climate in terrestrial ecosystems. Nature 2014; 514: 213-217.

Chan, S., Kendon, E., Fowler, H., Blenkinsop, S., Roberts, N., 2014. Projected increases in summer and winter UK sub-daily precipitation extremes from high-resolution regional climate models. Environ. Res. Lett. 9, 084019.

Chu, H., Fierer, N., Lauber, C.L., Caporaso, J., Knight, R., Grogan, P., 2010. Soil bacterial diversity in the Arctic is not fundamentally different from that found in other biomes. Environ. Microbiol. 12, 2998–3006.

Cosby, B., Ferrier, R., Jenkins, A., Wright, R., 2001. Modelling the effects of acid deposition: refinements, adjustments and inclusion of nitrogen dynamics in the MAGIC model. Hydrol. Earth Syst. Sci. 5, 499–518.

Curtin, D., Campbell, C., Jalil, A., 1998. Effects of acidity on mineralization: pH-dependence of organic matter mineralization in weakly acidic soils. Soil Biol. Biochem. 30, 57–64.

da Veiga, L.F., Grüning, B.A., Alves Aflitos, S., Röst, H.L., Uszkoreit, J., Barsnes, H., et al., 2017. BioContainers: an open-source and community-driven framework for software standardization. Bioinformatics 33, 2580–2582.

Desie, E., Vancampenhout, K., Heyens, K., Hlava, J., Verheyen, K., Muys, B., 2019. Forest conversion to conifers induces a regime shift in soil process domain affecting carbon stability. Soil Biol. Biochem. 136, 107540.

Doetterl, S., Stevens, A., Six, J., Merckx, R., Van Oost, K., Casanova Pinto, M., et al., 2015. Soil carbon storage controlled by interactions between geochemistry and climate. Nat. Geosci. 8, 780–783.

EuropeanCommission., 2023. Proposal for a Directive of the European Parliament and of the Council on Soil monitoring and Resilience. (soil Monitoring Law) 69.

Ewels, P.A., Peltzer, A., Fillinger, S., Patel, H., Alneberg, J., Wilm, A., et al., 2020. The nf-core framework for community-curated bioinformatics pipelines. Nat. Biotechnol. 38, 276–278.

Fernández-Calviño, D., Bååth, E., 2010. Growth response of the bacterial community to pH in soils differing in pH. FEMS Microbiol. Ecol. 73, 149–156.

Fernandez-Ugalde O, Scarpa S, Orgiazzi A, Panagos P, Van Liedekerke M, Marechal A, et al. LUCAS 2018 Soil Module. 2022.

Fierer, N., Jackson, R.B., 2006. The diversity and biogeography of soil bacterial communities. Proc. Natl. Acad. Sci. 103, 626–631.

Frazão, J., de Goede, R.G., Brussaard, L., Faber, J.H., Groot, J.C., Pulleman, M.M., 2017. Earthworm communities in arable fields and restored field margins, as related to management practices and surrounding landscape diversity. Agr Ecosyst Environ 248, 1–8.

Garforth, J., 2015. Lability and solubility of Ni, Cu, Zn, Cd and Pb in UK soils. University of Nottingham.

Griffiths, R.I., Thomson, B.C., James, P., Bell, T., Bailey, M., Whiteley, A.S., 2011. The bacterial biogeography of british soils. Environ. Microbiol. 13, 1642–1654.

Grüning, B., Dale, R., Sjödin, A., Chapman, B.A., Rowe, J., Tomkins-Tinch, C.H., et al., 2018. Bioconda: sustainable and comprehensive software distribution for the life sciences. Nat. Methods 15, 475–476.

Gubry-Rangin, C., Hai, B., Quince, C., Engel, M., Thomson, B.C., James, P., et al., 2011. Niche specialization of terrestrial archaeal ammonia oxidizers. Proc. Natl. Acad. Sci. 108, 21206–21211.

Hakonen, A., Hulth, S., Dufour, S., 2010. Analytical performance during ratiometric long-term imaging of pH in bioturbated sediments. Talanta 81, 1393–1401.

Hansen, P.M., Even, R., King, A.E., Lavalle, J., Schipanski, M., Cotrufo, M.F., 2024. Distinc, direct and climate-mediated environmental controls on global particulate and mineral-associated organic carbon storage. Glob. Chang. Biol. 30, e17080.

Hartemink, A.E., Barrow, N., 2023. Soil pH-nutrient relationships: the diagram. Plant and Soil 486, 209–215.

Hassani, A., Azapagic, A., Shokri, N., 2021. Global predictions of primary soil salinization under changing climate in the 21st century. Nat. Commun. 12, 6663.

Hernangómez, D., 2023. Using the tidyverse with terra objects: the tidyterra package. Journal of Open Source Software 8 (91), 5751.

Hijmans, R.J., 2020. terra: Spatial data analysis. Contributed Packages, CRAN.

Hirabayashi, Y., Kanae, S., 2009. First estimate of the future global population at risk of flooding. Hydrol. Res. Lett. 3, 6–9.

Hoeffner, K., Santonja, M., Monard, C., Barbe, L., Le Moing, M., Cluzeau, D., 2021. Soil properties, grassland management, and landscape diversity drive the assembly of earthworm communities in temperate grasslands. Pedosphere 31, 375–383.

Holmberg, M., Aherne, J., Austnes, K., Beloica, J., De Marco, A., Dirnböck, T., et al., 2018. Modelling study of soil C, N and pH response to air pollution and climate change using European LTER site observations. Sci. Total Environ. 640, 387–399.

Hou, D., 2023. Sustainable soil management for food security. Soil Use & Management 39.

Islam AKMS, Edwards DG, Asher CJ. pH optima for crop growth: results of a flowing solution culture experiment with six species. Plant and soil 1980; 54:339-357. Jenny H. Factors of soil formation: a system of quantitative pedology: Courier Corporation, 1994.

Jin, X., Kumar, L., Li, Z., Feng, H., Xu, X., Yang, G., et al., 2018. A review of data assimilation of remote sensing and crop models. Eur. J. Agron. 92, 141–152.

Jones, B., Goodall, T., George, P.B., Gweon, H.S., Puissant, J., Read, D.S., et al., 2021. Beyond taxonomic identification: integration of ecological responses to a soil bacterial 16S rRNA gene database. Front. Microbiol. 12, 682886.

Kharin, V.V., Zwiers, F.W., Zhang, X., Hegerl, G.C., 2007. Changes in temperature and precipitation extremes in the IPCC ensemble of global coupled model simulations. J. Clim. 20, 1419–1444.

Król, A., Mizerna, K., Bożym, M., 2020. An assessment of pH-dependent release and mobility of heavy metals from metallurgical slag. J. Hazard. Mater. 384, 121502.

Kundzewicz, Z.W., Kanae, S., Seneviratne, S.I., Handmer, J., Nicholls, N., Peduzzi, P., et al., 2014. Flood risk and climate change: global and regional perspectives. Hydrol. Sci. J. 59, 1–28.

Labouyrie, M., Ballabio, C., Romero, F., Panagos, P., Jones, A., Schmid, M.W., et al., 2023. Patterns in soil microbial diversity across Europe. Nat. Commun. 14, 3311.

Lakhani, K., Satchell, J., 1970:. Production by Lumbricus terrestris (L.). J. Anim. Ecol. 473–492.

Langeveld, J., Bouwman, A.F., van Hoek, W.J., Vilmin, L., Beusen, A.H., Mogollón, J.M., et al., 2020. Estimating dissolved carbon concentrations in global soils: a global database and model. SN Appl. Sci. 2, 1626.

Lebron, I., Suarez, D., Alberto, F., 1994. Stability of a calcareous saline-sodic soil during reclamation. Soil Sci. Soc. Am. J. 58, 1753–1762.

Lofts, S., 2022. POSSMs: a parsimonious speciation model for metals in soils. Environ. Chem. 18, 335–351.

Malik, A.A., Puissant, J., Buckeridge, K.M., Goodall, T., Jehmlich, N., Chowdhury, S., et al., 2018. Land use driven change in soil pH affects microbial carbon cycling processes. Nat. Commun. 9, 3591.

Martin, M., 2011. Cutadapt removes adapter sequences from high-throughput sequencing reads. Embnet. Journal 17, 10–12.

McBride, M., 1994. Environmental Chemistry of Soils Oxford Press. N. Y.

McCallum, H.M., Wilson, J.D., Beaumont, D., Sheldon, R., O'Brien, M.G., Park, K.J., 2016. A role for liming as a conservation intervention? Earthworm abundance is associated with higher soil pH and foraging activity of a threatened shorebird in upland grasslands. Agr Ecosyst Environ 223, 182–189.

Msimbira, L.A., Smith, D.L., 2020. The roles of plant growth promoting microbes in enhancing plant tolerance to acidity and alkalinity stresses. Front. Sustainable Food Syst. 4, 106.

Neina, D., 2019. The role of soil pH in plant nutrition and soil remediation. Appl. Environ. Soil Sci. 2019, 5794869.

Neirynck, J., Mirtcheva, S., Sioen, G., Lust, N., 2000. Impact of Tilia platyphyllos Scop., Fraxinus excelsior L., Acer pseudoplatanus L., Quercus robur L. and Fagus sylvatica L. on earthworm biomass and physico-chemical properties of a loamy topsoil. For. Ecol. Manage. 133, 275–286.

Orgiazzi, A., Ballabio, C., Panagos, P., Jones, A., Fernández-Ugalde, O., 2018. LUCAS Soil, the largest expandable soil dataset for Europe: a review. Eur. J. Soil Sci. 69, 140–153.

Page, K.L., Dang, Y.P., Martinez, C., Dalal, R.C., Wehr, J.B., Kopittke, P.M., Orton, T.G., Menzies, N.W., 2021. Review of crop-specific tolerance limits to acidity, salinity, and sodicity for seventeen cereal, pulse, and oilseed crops common to rainfed subtropical cropping systems. Land Degrad. Dev. 32, 2459–2480.

Panagos, P., Borrelli, P., Jones, A., Robinson, D.A., 2024. A 1 billion euro mission: A Soil Deal for Europe. Eur. J. Soil Sci. 75 (1), e13466.

Phillips, H.R., Bach, E.M., Bartz, M.L., Bennett, J.M., Beugnon, R., Briones, M.J., et al., 2021. Global data on earthworm abundance, biomass, diversity and corresponding environmental properties. Sci. Data 8, 136.

Piearce, T., 1972. Acid intolerant and ubiquitous Lumbricidae in selected habitats in North Wales. J. Anim. Ecol. 397–410.

Pozza, L., Field, D., 2020. The science of soil security and food security. Soil Secur. 1, 100002.

Puissant, J., Jones, B., Goodall, T., Mang, D., Blaud, A., Gweon, H.S., et al., 2019. The pH optimum of soil exoenzymes adapt to long term changes in soil pH. Soil Biol. Biochem. 138, 107601.
Quast, C., Pruesse, E., Yilmaz, P., Gerken, J., Schweer, T., Yarza, P., et al., 2012. The SILVA ribosomal RNA gene database project: improved data processing and web-based tools. Nucleic Acids Res. 41, D590–D596.
Reich, P.B., Oleksyn, J., Modrzynski, J., Mrozinski, P., Hobbie, S.E., Eissenstat, D.M., et al., 2005. Linking litter calcium, earthworms and soil properties: a common garden test with 14 tree species. Ecol. Lett. 8, 811–818.
Reinds, G.J., Van Oijen, M., Heuvelink, G.B., Kros, H., 2008. Bayesian calibration of the VSD soil acidification model using European forest monitoring data. Geoderma 146, 475–488.
Rengel, Z., 2011. Soil pH, soil health and climate change. Soil health and climate change. Springer 69–85.
Reynolds, B., Chamberlain, P., Poskitt, J., Woods, C., Scott, W., Rowe, E., et al., 2013. Countryside Survey: National "Soil Change" 1978–2007 for Topsoils in Great Britain—acidity, carbon, and total nitrogen status. Vadose Zone J. 12 (vzj2012), 0114.
Rinklebe, J., Shaheen, S.M., 2017. Redox chemistry of nickel in soils and sediments: a review. Chemosphere 179, 265–278.
Robinson, D.A., Hopmans, J.W., Filipovic, V., van der Ploeg, M., Lebron, I., Jones, S.B., et al., 2019. Global environmental changes impact soil hydraulic functions through biophysical feedbacks. Glob. Chang. Biol. 25, 1895–1904.
Robinson, D.A., Bentley, L., Jones, L., Feeney, C., Garbutt, A., Tandy, S., Lebron, I., Thomas, A., Reinsch, S., Norton, L., Maskell, L., 2024. Five decades' experience of long-term soil monitoring, and key design principles, to assist the EU soil health mission. Eur. J. Soil Sci. 75, e13570.
Rowell DL. "Soil acidity and alkalinity." In Russell's soil conditions and plant growth. Eleventh edition 1988, 844-898 ref. 175 editor A Wild.
Roy RN, Finck A, Blair GJ, Tandon HLS. Plant nutrition for food security. A guide for integrated nutrient management. FAO Fertilizer and Plant Nutrition Bulletin 2006; 16:201-214. Schelfhout S, Mertens J, Verheyen K, Vesterdal L, Baeten L, Muys B, et al. Tree species identity shapes earthworm communities. Forests 2017; 8: 85.
Schulz-Zunkel, C., Rinklebe, J., Bork, H.-R., 2015. Trace element release patterns from three floodplain soils under simulated oxidized–reduced cycles. Ecol. Eng. 83, 485–495.
Seaton, F.M., George, P.B., Lebron, I., Jones, D.L., Creer, S., Robinson, D.A., 2020. Soil textural heterogeneity impacts bacterial but not fungal diversity. Soil Biol. Biochem. 144, 107766.
Seaton, F.M., Robinson, D.A., Monteith, D., Lebron, I., Bürkner, P., Tomlinson, S., et al., 2023. Fifty years of reduction in sulphur deposition drives recovery in soil pH and plant communities. J. Ecol. 111, 464–478.
Seaton, F.M., George, P.B., Alison, J., Jones, D.L., Creer, S., Smart, S.M., et al., 2024. A diversity of diversities: do complex environmental effects underpin associations between below-and above-ground taxa? J. Ecol. 112, 1550–1564.
Shainberg, I., Levy, G., 2020. Physico-chemical effects of salts upon infiltration and water movement in soils. Interacting processes in soil science. CRC Press 37–93.
Slessarev, E., Lin, Y., Bingham, N., Johnson, J., Dai, Y., Schimel, J., et al., 2016. Water balance creates a threshold in soil pH at the global scale. Nature 540, 567–569.
Smith, P., Poch, R.M., Lobb, D.A., Bhattacharyya, R., Alloush, G., Eudoxie, G.D., et al., 2024. Status of the World's Soils. Annu. Rev. Env. Resour. 49.
Stocker, T.F., 2015. Implications of climate science for negotiators. FERDI Working Paper.
Straub, D., Blackwell, N., Langarica-Fuentes, A., Peltzer, A., Nahnsen, S., Kleindienst, S., 2020. Interpretations of environmental microbial community studies are biased by the selected 16S rRNA (gene) amplicon sequencing pipeline. Front. Microbiol. 11, 550420.
Team RC. Package 'parallel'. 2024.
Thompson, A., Chadwick, O.A., Rancourt, D.G., Chorover, J., 2006. Iron-oxide crystallinity increases during soil redox oscillations. Geochim. Cosmochim. Acta 70, 1710–1727.
Tockner, K., Lorang, M.S., Stanford, J.A., 2010. River flood plains are model ecosystems to test general hydrogeomorphic and ecological concepts. River Res. Appl. 26, 76–86.
Tóth, G., Hermann, T., Szatmári, G., Pásztor, L., 2016. Maps of heavy metals in the soils of the European Union and proposed priority areas for detailed assessment. Sci. Total Environ. 565, 1054–1062.
Tripathi, B.M., Kim, M., Singh, D., Lee-Cruz, L., Lai-Hoe, A., Ainuddin, A., et al., 2012. Tropical soil bacterial communities in Malaysia: pH dominates in the equatorial tropics too. Microb. Ecol. 64, 474–484.
Turner, B.L., Romero, T.E., 2010. Stability of hydrolytic enzyme activity and microbial phosphorus during storage of tropical rain forest soils. Soil Biol. Biochem. 42, 459–465.
Van Breemen, N., Mulder, J., Driscoll, C., 1983. Acidification and alkalinization of soils. Plant and Soil 75, 283–308.
van der Sloot, H.A., van Zomeren, A., 2012. Characterisation leaching tests and associated geochemical speciation modelling to assess long term release behaviour from extractive wastes. Mine Water Environ. 31, 92–103.
Van Eynde, E., Fendrich, A.N., Ballabio, C., Panagos, P., 2023. Spatial assessment of topsoil zinc concentrations in Europe. Sci. Total Environ. 892, 164512.
Vitousek, P.M., Ladefoged, T.N., Kirch, P.V., Hartshorn, A.S., Graves, M.W., Hotchkiss, S. C., et al., 2004. Soils, agriculture, and society in precontact Hawaii. Science 304, 1665–1669.
Wallman, P., Svensson, M.G., Sverdrup, H., Belyazid, S., 2005. ForSAFE—an integrated process-oriented forest model for long-term sustainability assessments. For. Ecol. Manage. 207, 19–36.
Wang, C., Kuzyakov, Y., 2024. Soil organic matter priming: the pH effects. Glob. Chang. Biol. 30, e17349.
Were, K., Bui, D.T., Dick, Ø.B., Singh, B.R., 2015. A comparative assessment of support vector regression, artificial neural networks, and random forests for predicting and mapping soil organic carbon stocks across an Afromontane landscape. Ecol. Ind. 52, 394–403.
Wickham H, Wickham H. Toolbox. ggplot2: Elegant Graphics for Data Analysis 2016: 33-74.
Wood, S.N., 2011. Fast stable restricted maximum likelihood and marginal likelihood estimation of semiparametric generalized linear models. J. R. Stat. Soc. Ser. B Stat Methodol. 73, 3–36.
Xiao, S., Ou, M., Geng, Y., Zhou, T., 2023. Mapping soil pH levels across Europe: an analysis of LUCAS topsoil data using random forest kriging (RFK). Soil Use Manag. 39, 900–916.
Yu, W., Weintraub, S.R., Hall, S.J., 2021. Climatic and geochemical controls on soil carbon at the continental scale: interactions and thresholds. Global Biogeochem. Cycles 35, e2020GB006781.
Zeng, M., de Vries, W., Bonten, L.T., Zhu, Q., Hao, T., Liu, X., et al., 2017. Model-based analysis of the long-term effects of fertilization management on cropland soil acidification. Environ. Sci. Technol. 51, 3843–3851.
Zhao, X., Yang, Y., Shen, H., Geng, X., Fang, J., 2019. Global soil–climate–biome diagram: linking surface soil properties to climate and biota. Biogeosciences 16, 2857–2871.
Zhou, X., Tahvanainen, T., Malard, L., Chen, L., Pérez-Pérez, J., Berninger, F., 2024. Global analysis of soil bacterial genera and diversity in response to pH. Soil Biol. Biochem. 198, 109552.